DYE-SENSITIZED SOLAR CELLS USING PHTHALOYLCHITOSAN BASED GEL POLYMER ELECTROLYTE CONTAINING I^-/I_3^- REDOX SPECIES

SHAHAN SHAH

FACULTY OF SCIENCE
UNIVERSITY OF MALAYA
KUALA LUMPUR

2016

University of Malaya

DYE-SENSITIZED SOLAR CELLS USING PHTHALOYLCHITOSAN BASED HEL POLYMER ELECTROLYTE CONTAININNG I^-/I_3^- REDOX SPECIES

SHAHAN SHAH

DISSERTATION SUBMITTED IN FULFILMENT OF THE REQUIREMENTS FOR THE DEGREE OF MASTER OF SCIENCE

FACULTY OF SCIENCE
UNIVERSITY OF MALAYA
KUALA LUMPUR

2016

University of Malaya

UNIVERSITY OF MALAYA

ORIGINAL LITERARY WORK DECLARATION

Name of Candidate: Shahan Shah

Matric No: SGR 120115

Name of Degree: Master of Science

Title of Project Paper/Research Report/Dissertation/Thesis ("this Work"):

Dye-sensitized solar cells using Phthaloyalchitosan based gel polymer electrolyte containing I^-/I_3^- redox species

Field of Study: Advanced materials

I do solemnly and sincerely declare that:

(1) I am the sole author/writer of this Work;
(2) This Work is original;
(3) Any use of any work in which copyright exists was done by way of fair dealing and for permitted purposes and any excerpt or extract from, or reference to or reproduction of any copyright work has been disclosed expressly and sufficiently and the title of the Work and its authorship have been acknowledged in this Work;
(4) I do not have any actual knowledge nor do I ought reasonably to know that the making of this work constitutes an infringement of any copyright work;
(5) I hereby assign all and every rights in the copyright to this Work to the University of Malaya ("UM"), who henceforth shall be owner of the copyright in this Work and that any reproduction or use in any form or by any means whatsoever is prohibited without the written consent of UM having been first had and obtained;
(6) I am fully aware that if in the course of making this Work I have infringed any copyright whether intentionally or otherwise, I may be subject to legal action or any other action as may be determined by UM.

Candidate's Signature Date:

Subscribed and solemnly declared before,

Witness's Signature Date:

Name:

Designation:

University of Malaya

ABSTRACT

Gel polymer electrolytes (GPE) consisting of phthaloylchitosan (PhCh), polyethylene oxide (PEO), dimethylformamide (DMF), ethylene carbonate (EC),tetrapropyl ammonium iodide (TPAI) and iodine (I_2) have been prepared and characterized using electrochemical impedance spectroscopy (EIS). The highest conductivity of 11.1 mS cm^{-1} was obtained for 5.04 wt.% PhCh-1.26 wt.% PEO-31.51 wt.% DMF-37.81wt.% EC-22.68wt.% TPAI-1.7 wt. % I_2 GPE. Dye-sensitized solar cell (DSSCs) have been fabricated by sandwiching GPE between FTO/TiO_2-dye photoanode and platinum/FTO counter electrode. The photocurrent density-voltage (*J-V*) characteristics of the DSSCs have been measured under white light illumination of 100 W m^{-2} with active area of 0.20 cm^2. The optimized GPE exhibits the efficiency of 7.1 % using N3 dye as sensitizer and 0.81 % with mixed natural dyes. The natural dyes used were anthocyanin (An) and chlorophyll (Chl) which have been extracted from black rice and fragrant screwpine (*Pandanus amaryllifolius*) leave, respectively using methanol as solvent. The anthocyanin and chlorophyll dyes were characterized using UV-Vis absorption spectroscopy. While the anthocyanin dye has a broader absorption peak at 541 nm, the chlorophyll dye has two prominent absorption peaks at 410 nm and 663 nm. The anthocyanin and chlorophyll dyes were deposited sequentially on the TiO_2 electrode. The optimized GPE has been added with tert-butyl-pyridine (TBP) at different concentration as additives and have been tested in DSSC. With the addition of 8 wt. % of TBP, the conductivity of GPE decreased to 10.28 mS cm^{-1}. However,the open circuit voltage, (V_{oc}) and the efficiency of DSSC using 8 wt. % TBP increased to 0.73 V and 8.84 %, respectively.

University of Malaya

ABSTRAK

Elektrolit gel polimer (GPE) yang terdiri daripada phthaloylchitosan (PhCh); polyethylene oksida (PEO); dimethylformamide (DMF); ethylene karbonat (EC); dan iodin (I_2) telah disediakan dan dicirikan menggunakan spektroskopi impedans elektrokimia (EIS). Kekonduksian tertinggi 11.1 mS cm^{-1} telah diperolehi bagi 5.04 wt.% PhCh-1.26 wt.% PEO-31.51 wt.% DMF-37.81 wt.% EC-22.68wt.% TPAI-1.7 wt. % I_2 GPE. DSSCs telah difabrikasi dengan meletakkan GPE di antara FTO/TiO_2-pencelup/ dan platinum/FTO. Pencirian ketumpatan arus-voltan (*J-V*) bagi DSSCs telah diukur di bawah pencahayaan cahaya putih 1000 W m^{-2} dengan keluasan aktif 0.20 cm^2. DSSC yang menggunakan GPE yang telah dioptimumkan memberikan kecekapan sebanyak 7.1 % bagi pencelup N3 dan 0.81 % bagi pencelup semulajadi. Pencelup semulajadi yang digunakan adalah antosianin (An) dan klorofil (Chl) yang telah diekstrak daripada pulut hitam dan daun pandan (*Pandanus amaryllifolius*) dengan menggunakan metanol sebagai pelarut. Pencelup antosianin dan klorofil dicirikan menggunakan Penyerapan UV-Vis spektroskopi . Pencelup antosianin mempunyai penyerapan puncak yang lebih luas pada 541 nm, manakala pencelup klorofil mempunyai dua puncak penyerapan yang jelas kelihatan di 410 nm dan 663 nm. Pencelup antosianin dan klorofil telah dideposit kan secara berurutan pada elektrod TiO_2. GPE yang dioptimumkan juga telah ditambahkan dengan tertbutyl pyridine (TBP) pada kepekatan yang berbeza sebagai bahan tambahan dan diuji dalam DSSC. Dengan penambahan 8 wt. % TBP, kekonduksian GPE turun kepada 10.28 mS cm^{-1}. Walau bagaimanapun dan voltan litar terbuka, (V_{oc}) dan dengan kecekapan DSSC masing-masing meningkat kepada 0.73 V dan 8.84 %.

University of Malaya

ACKNOWLEDGEMENTS

Carried out of this dissertation successfully, I would like to express my solely gratitude to Almighty Allah. Firstly, I would like to tribute my appreciation to my supervisors; Professor Dr. Abdul Kariem Arof for the guidance and strong commitment that he have given along with mentoring me to complete my project profoundly. Thank you very much from my bottom of my heart for all your support and dedications in perfecting this project. In addition, I would like to express my cordially thanks to my second supervisor; Dr. Hamdi Ali @ Buraidah who helped me with productive ideas in nourishment this project to complete. Without their outstanding contribution, this research may not be completed. Besides that, thanks to all my lab friends of centre for Ionics, University of Malay. Special thanks to Dr. Teo Li Ping, Dr. Thompson Woo, Dr Sim Lina, Dr. Rusi, Dr.Jun Hieng Kiat, Dr, Wendy liew,Pei yi Chan, Mr. Ismail ,Ammar, Syahmi,Khairil, Kim, Dr. Ikwan Syafiq mohd Noor and Wan. I also would like to thank to University of Malaya for PPP research grant. Finally, I wish to express my heartily gratitude to my family members specially my younger sister Amrina Akter for their support, encouragement and supporting which led to the successes of this project.

Shahan Shah

29 November 2016

University of Malaya

TABLE OF CONTENTS

CONTENT		Page
Declaration		ii
Abstract		iii
Abstrak		iv
Acknowledgement		v
Table of Contents		vi
List of Figures		ix
List of Tables		xi
Abbreviations		xii
CHAPTER 1: INTRODUCTION		1
1.1	Background	1
1.2	Problem Statement	4
1.3	Objectives of the Thesis	5
1.4	Scope of the dissertation	5
CHAPTER 2: REVIEW OF LITERATURE		7
2.1	Introduction	7
2.2	Basic Structure of DSSCs	7
2.3	Working Principles of DSSCs	8
2.4	Photovoltaic Parameters of DSSC	10
2.5	Components of DSSCs	12
2.6	Conducting Glass Substrates	13
2.7	Photoanode: The TiO_2 Layer	13
2.8	Counter Electrode	14
2.9	Liquid electrolytes	15
2.9.1	Organic Solvent	16
2.9.2.	Redox Couple	16
2.9.3.	Additives	17
2.10	Polymer Electrolytes in DSSCs	18
2.11	Dye as Sensitizer	19
2.11.1	Ruthenium (Ru) dye	19
2.11.2	Organic Dyes	20
2.11.3	Natural Dye Sensitizers	21
2.11.4	Flavonoid	25

University of Malaya

2.11.5 Carotenoid 26
2.11.6 Chlorophyll 27
2.12 The Dye Anchoring on the TiO_2 Semiconductor 27
2.13 Combining Sensitizers 28
2.14 Summary 29
CHAPTER 3: EXPERIMENTAL METHODS 30
3.1 Introduction 30
3.2 Materials 30
3.3 Electrode Preparation 31
3.3.1 Glass Substrate Washing Process 31
3.3.2 TiO_2 Photoelectrode Preparation 31
3.4 Dye Solution Preparation 31
3.5 Counter Electrode Preparation 32
3.6 Preparation of Gel Polymer Electrolytes 32
3.7 Fabrication of DSSCs 33
3.8 Characterization Techniques 34
3.8.1 UV-Vis Spectroscopy 34
3.8.2 Electrochemical Impedance Spectroscopy (EIS) 34
3.8.3 Incident Photon-to-Current Efficiency (IPCE) 36
3.9 Summary 36
CHAPTER 4: RESULTS AND DISCUSSION (PhCh-PEO-DMF-EC-TPAI-I_2) 37
4.1 Introduction 37
4.2 The electrical conductivity of PhCh-PEO-DMF-EC-TPAI-I_2 electrolytes 37
4.3 *J-V* Characteristics of DSSCs using PhCh-PEO-DMF-EC-TPAI-I_2 electrolytes 41
4.4 Incident Photon to Current Conversion Efficiency (IPCE) of DSSCs using PhCh-PEO-DMF-EC-TPAI-I_2 electrolytes 43
4.5 Electrochemical Impedance Spectroscopy (EIS) on DSSCs using PhCh-PEO-DMF-EC-TPAI-I_2 electrolytes 44
4.6. Natural Dyes as Sensitizer 45
4.7. Summary 50
CHAPTER 5: RESULTS AND DISCUSSION (PhCh-PEO-DMF-EC-TPAI-I_2-TBP) 51

University of Malaya

5.1. Introduction 51
5.2. The electrical conductivity of PhCh-PEO-DMF-EC-TPAI-I_2-TBP electrolytes 51
5.3. *J-V* Characteristics of DSSCs using PhCh-PEO-DMF-EC-TPAI-I_2-TBP electrolytes 54
5.4. Incident Photon to Current Conversion Efficiency (IPCE) of DSSCs using PhCh-PEO-DMF-EC-TPAI-I_2-TBP electrolytes 56
5.5. Electrochemical Impedance Spectroscopy (EIS) on DSSCs using PhCh-PEO-DMF-EC-TPAI-I_2-TBP electrolytes 57
5.6. Summary 59
CHAPTER 6: CONCLUSION AND SUGGESTIONS FOR FUTURE WORK 60
REFERENCES 61
LIST OF PUBLICATION 73

University of Malaya

LIST OF FIGURES

Figures	Captions	Page
Figure 1.1	The images of different renewable energy sources	2
Figure 1.2	Solar radiation spectrum (Shockley *et al.,* 1961)	3
Figure 1.3	Image of silicon based solar cell setup: location archive building at the Penang Free School, Penang, Malaysia	4
Figure 2.1	Schematic representation of a DSSC O'Regan and Gräetzel (1991)	8
Figure 2.2	The working principles of DSSC	9
Figure 2.3	A typical current-voltage (I-V) curve of a DSSC	11
Figure 2.4	The major component of DSSC	12
Figure 2.5	The structure of some of high performance Ru-metal based dye molecules with their efficiencies (Nazzeruddin *et al.,* 1993)	20
Figure 2.6	(a) Donor-p-acceptor structure principle of an organic dye in DSSCs with TiO_2 photoanodes (Nazzeruddin *et al.,* 1993),(b) Possible binding modes of a COOH-group to TiO_2.(Pan *et al*.,2002)	21
Figure 2.7	Binding modes for carboxylate unit on TiO_2 surface (Deacon and Phillips, 1980)	28
Figure 3.1	Image of fabricated DSSCs	34
Figure 3.2	(a) Nyquist plot, imaginary part of the impedance, *Z"*, versus its real part, *Z'*, (b) Bode plot, absolute value of the impedance, $\lvert Z \rvert$, versus the frequency, and (c) Bode plot, phase angle, φ, versus the frequency	35
Figure 4.1	Nyquist plots of PhCh-PEO-DMF-EC-TPAI-I_2 GPE	39
Figure 4.2	Conductivity-temperature dependence of gel polymers electrolytes	40
Figure 4.3	Graph of activation energy vs TPAI salt contents	41
Figure 4.4	*J-V* curves of DSSCs with various amount of TPAI	42
Figure 4.5	IPCE curves of DSSCs with various amount of TPAI salt	43
Figure 4.6	Nyquist plots of DSSCs with various amount of TPAI salt	44
Figure 4.7	UV-vis absorbance curves of anthocyanin dyes	46
Figure 4.8	UV-vis absorbance curves of chlorophyll dyes	46

University of Malaya

Figure 4.9	*J-V* curves of DSSCs with batch A and batch B photoelectrodes	47
Figure 4.10	IPCE curves of Na1, Na2, Na3 and Na4 cells	48
Figure 4.11	The EIS plots of Na1, Na2, Na3 and Na4 cells	49
Figure 5.1	Nyquist plot of PhCh-PEO-DMF-EC-TPAI-I_2-TBP GPE	52
Figure 5.2	Conductivity of gel polymer electrolytes at different temperatures	53
Figure 5.3	*J-V* curves of DSSCs with TBP	54
Figure 5.4	IPCE curves of DSSCs with various amount of TBP	56
Figure 5.5	Nyquist graphs of solar cells	58

University of Malaya

LIST OF TABLES

Tables	Captions	Page
Table 2.1	Physical properties of some organic solvents (Brand Tech Scientific, Inc.)	16
Table 2.2	Some chemical structures of the natural dyes (Furukawa *et al* 2009)	22
Table 3.1	Electrolytes composition for first system and its designation	33
Table 3.2	Electrolytes composition (in gram) for second system and its designation	33
Table 3.3	Electrolytes composition (in wt.%) for second system and its designation	33
Table 4.1	Photovoltaic parameters of DSSCs fabricated with various amount of TPAI	42
Table 4.2	EIS parameters of DSSCs	45
Table 4.3	Performance parameters of DSSCs with batch A and B photoelectrodes	48
Table 4.4	EIS parameters of DSSCs with batch A and B	50
Table 5.1	Photovoltaic performance parameters of DSSCs with various amount of TBP	55
Table 5.2	The R1, R2 and R3 values for the DSSCs with various amount of TBP	59

University of Malaya

ABBREVIATIONS

UV	Ultraviolet
IR	Infrared
DSSC	Dye-sensitized solar cell
CIGS	Copper indium gallium diselenide
CdTe	Cadmium telluride
QDSSC	Quantum dot sensitized solar cell
EIS	Electrochemical impedance spectroscopy
J-V	Photo current density
TPAI	Tetrapropyl ammonium iodide
V_{oc}	Photovoltage
J_{sc}	Short circuit current
FF	Fill factor
η	Efficiency
CE	Counter electrode
ACN	Acetonitrile
DMF	Dimethyl formamide
DMSO	Dimethyl sulfoxide
PC	Propylene carbonate
EC	Ethylene carbonate
NMP	*n*-methyl-2-pyrolidone
TBP	Tertbutyl pyridine
Chl	Chlorophyll
An	Anthocyanin
Mg	Magnesium
-COOH	Carboxylic
$-SO_3^-$	Sulfonate
N3	Ruthenium metal dye
GPE	Gel polymer electrolyte
PhCh	Phthaloylchitosan
PEO	Polyethylene oxide
I_2	Iodine
IPCE	Incident photon to current conversion efficiency

University of Malaya

FTO	Fluorine-doped tin oxide
ITO	Indium-doped tin oxide
HOMO	Highest occupied molecular orbital
LUMO	Low unoccupied molecular orbital
CB	Conduction band

University of Malaya

CHAPTER 1: INTRODUCTION

1.1 Background

Energy is one of the most fundamental parts of our universe. It plays a vital role in the development of mankind. The sources of all conventional energies are non-renewable. These include coal, petroleum, natural gas and so on which have been used from the very beginning of human civilization. These energy are being used everywhere and the total reserves has been largely depleted. Discovering and exploiting new resources has become an increasingly difficult task. It has been predicted that deposits of petroleum and coal in fossil banks will get exhausted in the near future. The burning of fossil fuels to create energy can cause air and water contamination in the environment (Nature Reports Climate Change, 2008). More importantly, a lot of heat is being added to our earth due to emission of CO_2 from burning of fossil fuels that has contributed to global change.

Nowadays, research on energy is focusing on green technology. Green implying the technology produces "clean energy" without polluting the environment. The reserve derived from the conversion of oil, coal and gas constitutes approximately 36%, 27% and 23% respectively (International Energy Outlook, 2013). The balance is from the other sources. Renewable energy sources have had a great impact on growing energy demand due to the fast depletion of fossil fuels. Renewable energy sources are also known as regenerated resources. These include geothermal heat, hydro, wind and the most abundant solar energy. The different types of renewable energy sources are shown in Figure 1.1. Among the sources of renewable energy, solar energy is the most available and cleanest renewable energy. Sunlight is a mixture of electromagnetic wave comprising of infrared, visible, and ultraviolet light. The solar spectrum is approximately similar to the black body radiation, which is shown in Figure 1.2. Solar generated energy can be a significant application for future generation due to its most abundance and availability. The total

University of Malaya

energy supply to earth from the sun is 3×10^{24} joules a year (Nazzerruddin *et al*., 1993, Rajendran *et al*,. 2002). 0.1 % of this energy is converted for use, it amounts to about four times of the world's energy production in a year. Hence, among the various renewable energy technology solar photovoltaics 'in particular' have gained much attention to solve energy related problems without any environmental pollution.

The efficiency of a photovoltaic is dependent mainly on the energy distribution and intensity of the incident light. Solar distribution may be different in different areas. This depends on many factors such as Earth/Sun distance and rotation, weather, geographical location, shiny day conditions. An accurate power density and standard solar spectrum will enable comparison among all solar devices to be made. The emission wavelength range covers from the ultraviolet (UV) to visible and infrared (IR) regions at around 500 nm (Voigt *et al.*, 2002).

Figure 1.1. The images of different renewable energy sources.

University of Malaya

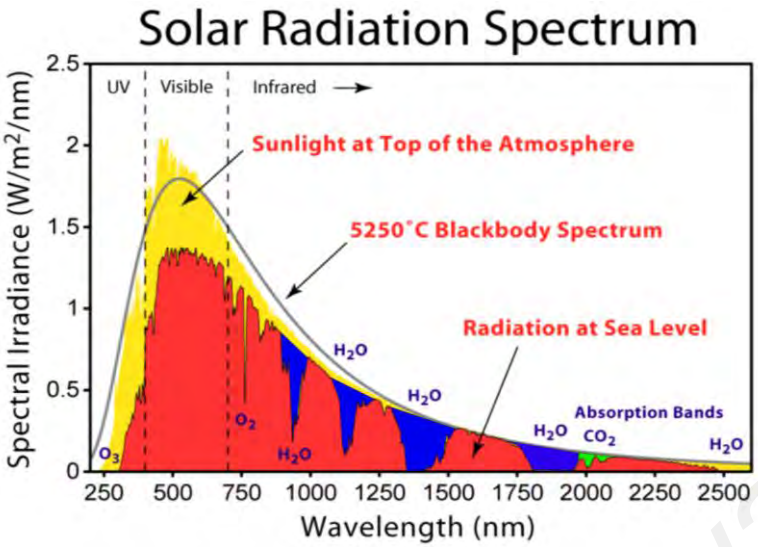

Figure 1.2. Solar radiation spectrum (Shockley *et al.,* 1961).

The semiconductor material is a major component in solar energy to electricity conversion devices. There are three different generations of photovoltaics. The limitation of solar conversion efficiency for both first and second generation is not more than 31% power efficiency limited by the Schockley-Queisser effect (Shockley *et al.,* 1961). It is noted that the band gap energy of the semiconductor materials must not be lower than the photons energy.

Solar cells work when they absorb photons from sunlight and electrons start to flow after completing circuit in between two poles (Green, 1982). The dye-sensitized solar cell (DSSC) technology has shown the possibility of producing renewable energy using natural material. Today we have benefited either in industrial or domestic sector using solar energy over the world.

Solar cells have been classified according to the semiconducting materials used. Most cells are made from silicon, which is doped to release electrons after exposure to sunlight. Figure 1.3 shows a typical silicon based solar cell used on roof.

Until today three generations of solar cells can be used according to our needs. These are categorized as below.

University of Malaya

First generation solar cells: Silicon based first generation photovoltaics have still better quality over other types of solar cells in the commercial market. These crystalline silicon wafer cells consist of multi crystalline ribbons.

Second generation solar cells: These cells are termed as thin film solar cell. There are four types namely amorphous silicon cells, polycrystalline silicon cells, copper indium gallium diselenide (CIGS) alloy cells and cadmium telluride (CdTe) cells. Their band gap varies from 1.38 eV to about 1.7 eV.

Third generation solar cells: The example of these type of photovoltaic systems are dye sensitized solar cell (DSSCs), quantum dot sensitized solar cell (QDSSC), organic solar cell, perovskite solar cell and etc.

Figure 1.3. Image of silicon based solar cell setup: location archive building at Penang Free School, Penang, Malaysia.

1.2 Problem statement

In the DSSC application, the highest solar cell efficiency was obtained using liquid electrolytes. In spite of highly efficiencies of DSSCs, the liquid electrolytes have many problems such as leakage, evaporation, corrosive and etc. In order to overcome these problem, gel polymer electrolyte have been studied and applied in DSSCs. The gel polymer electrolytes can be made through the process of polymerization or dispersion of

Universiti Malaya

polymeric materials with salt complexes (Hagfeldt *et al.,* 2010). Gel polymer electrolytes have high mechanical stability as well as low electrical conductivity compared with liquid electrolytes.

1.3 Objectives of the thesis

This dissertation is about dye-sensitized solar cells (DSSCs) using biopolymer phthaloychitosan based gel polymer electrolytes.

The major objectives of this work are as follows:

a) To investigate the effect of tetrapropyl ammonium iodide concentration on the conductivity of gel polymer electrolyte.

b) To identify the potentiality of fragrant screwpine (*Pandanus amaryllifolius*) and black rice as natural sensitizers.

c) To acculturate how solar cell efficiency can be increased by incorporating additive i.e. tert-butyl-pyridine (TBP) in polymer electrolytes.

1.4 Scope of the dissertation

This dissertation is made of 6 chapters. Chapter 1 introduces the dissertation and its contents as well as problem statement and objectives. Chapter 2 is an inexhaustive overview on the working principle of dye sensitized solar cell (DSSCs), natural dyes commonly used in DSSCs as well as the selection of materials used in the fabrication of DSSCs. Chapter 3 describes the details of electrolyte preparation, anthocyanin and chlorophyll extraction and optical characterization i.e. UV-vis absorption spectroscopy of the dye solution and electrochemical impedance spectroscopy (EIS). The chapter also deals with DSSC fabrications and characterization.

University of Malaya

Chapter 4 illustrates the influence of tetrapropyl ammonium iodide (TPAI) added to the phthaloylchitosan based gel polymer electrolyte and the photovoltaic performance of DSSCs using the N3 dye and natural dyes (anthocyanin and chlorophyll) as sensitizers. Chapter 5 describes the effect on solar cell performance using gel polymer electrolyte added with tert-butyl pyridine. Finally, chapter 6 discusses all the results and concludes the dissertation with some suggestions for the future work.

University of Malaya

CHAPTER 2: REVIEW OF LITERATURE

2.1 Introduction

The photovoltaic devices called Dye Sensitized Solar Cell (DSSCs) constructed on nano-crystalline TiO_2 were developed by O'Regan and Gräetzel (1991). This type of solar cell is featured by their relatively high efficiency (11% at full sunlight) and low fabrication cost (1/10th to 1/5th of silicon solar cells) Gräetzel (1995). Since the birth of DSSCs, great efforts have been devoted in making these devices more efficient and stable. Long-term stability tests show good prospects of DSSCs for domestic devices and decorative applications. They have attracted considerable interest since the cells are fabricated with the easily obtainable raw materials and comparably low cost and facile fabrication techniques. This chapter fully deals the review of literature with fundamentals and formation of DSSC.

2.2 Basic structure of DSSCs

DSSC consists of four components. This includes a photoelectrode of nanostructured semiconductor (usually TiO_2) attached to the conducting substrate (TCO), a dye monolayer adsorbed on the semiconductor surface , electrolyte (typically with I^-/I_3^- mediator) and a platinized FTO counter electrode or cathode. Figure 2.1 shows the structure of the DSSC.

University of Malaya

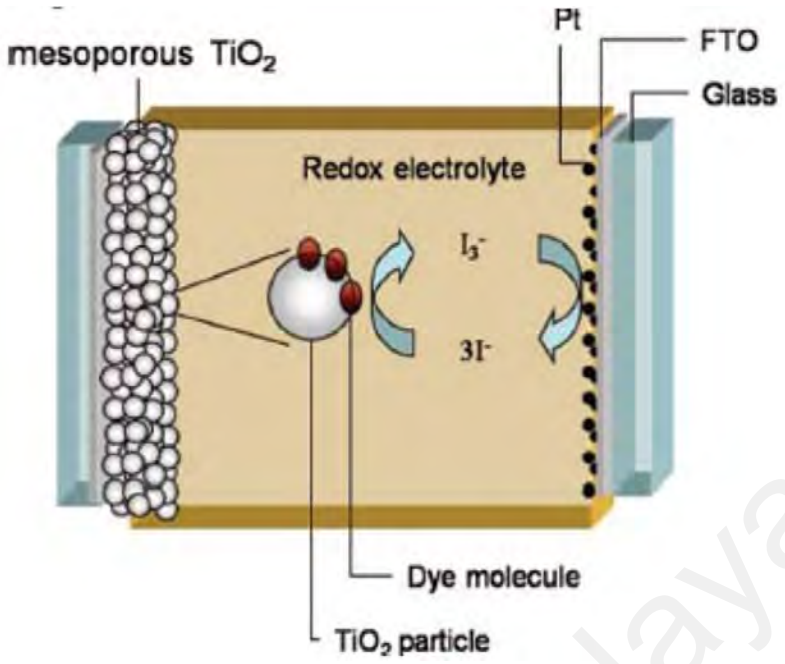

Figure 2.1. Schematic representation of a DSSC O'Regan and Gräetzel (1991).

2.3 Working principles of DSSCs

The photoanode of a DSSC or Gräetzel cell is made of semiconductor such as TiO_2, ZnO, SiO_2 etc., a monolayer of dye molecule adsorbed on it, an iodide/triiodide couple dissolved in an ions conducting medium and a platinum (Pt) or carbon (C) etc., coated conducting substrate as cathode. Then, these two electrodes are connected by an external circuit in order to offer a pathway to electricity. The DSSC uses the same basic principle as plant photosynthesis to generate electrical energy from the solar energy. Each plant leaf is a photochemical cell that converts the solar energy into biological materials. Although only 0.02 % to 0.05 % of the incident energy is converted by the photosynthesis process, the food being produced is 100 times more than what is needed for mankind. The chlorophyll in green leaves generate electrons using the photon energy which triggers the subsequent reactions to complete the photosynthesis process. Hence, conversion of photon for DSSCs is an artificial photosynthesis process. The working configuration of DSSC is demonstrated in Figure 2.2.

University of Malaya

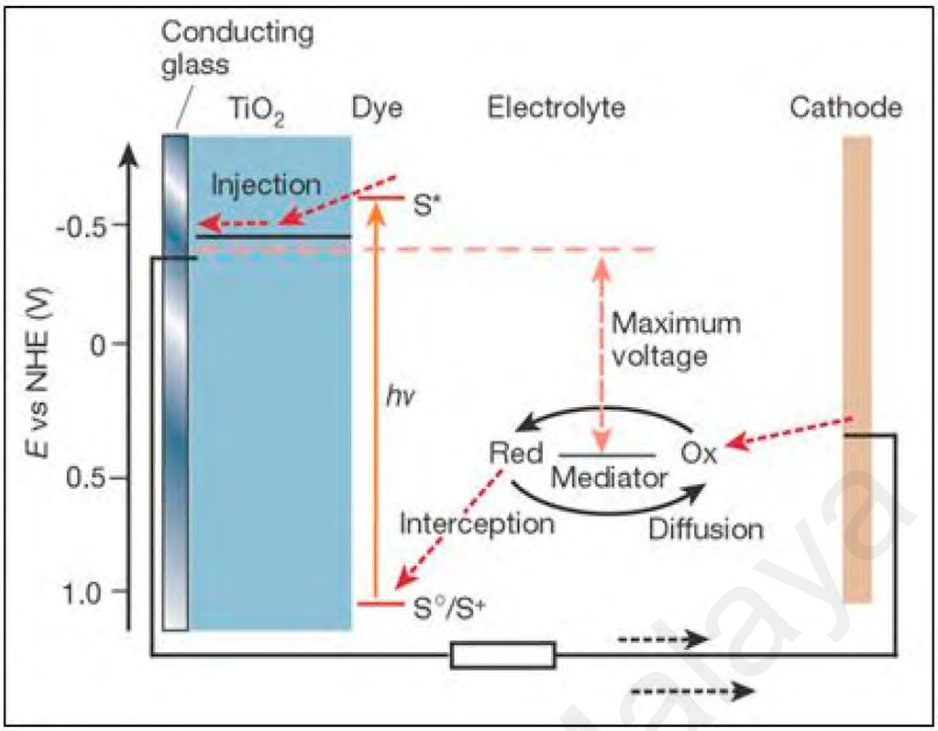

Figure 2.2. The working principles of DSSC.

When the dye loaded photoanode is illuminated, the dye molecules (D) get excited when they absorb photons. The excited dye molecule will be oxidized and electrons released enters the TiO_2 semiconductor. The electrons then exit the photoanode and move to the cathode through the external circuit where they reduce triiodide ions into iodide ions. The iodide ion diffuses towards the dye and releases an electron to the oxidized dye. The dye gets regenerated and the iodide ion is oxidized into a triiodide ion again. The electron circuit is complete and the cycle repeats itself. Electricity is thus generated. The above process in DSSC is given by the following reactions.

Upon absorbing incident photon by the dye, the dye molecules get excited an electron from ground state $\mathbf{S°}$ to a higher lying excited state $\mathbf{S^*}$.

$$\mathbf{S°} + h\upsilon \rightarrow \mathbf{S^*} \qquad (2.1)$$

Here, h is Planck's constant, v is light frequency

From the state of elevated energy, $\mathbf{S^*}$ an electron is injected into the TiO_2 nanoparticle network and the dye molecule oxidized to $\mathbf{S^+}$.

University of Malaya

$$S^* + TiO_2 \rightarrow S^+ + e^-(TiO_2) \quad (2.2)$$

For an electrolyte with I_3^-/I^- mediator (Theerthagiri *et al.*, 2015), the electron that has reached the counter electrode reduces the triiodide ion (equation 2.3).The I^- ion diffuses towards the dye where it releases an electron and becomes oxidized. The electron is accepted by the oxidized dye and is regenerated (equation 2.4).

$$I_3^- + 2e^- \rightarrow 3I^- \quad (2.3)$$

$$2S^+ + 3I^- \rightarrow 2S^\circ + I_3^- \quad (2.4)$$

It is to be noted that the injected electrons from the dye can recombine with I_3^- ions and contribute to dark current.

$$I_3^- + 2e^-(TiO_2) \rightarrow 3I^- \quad (2.5)$$

The recombination is also possible between the injected electrons and the oxidized dyes.

$$S^+ + e^-(TiO_2) \rightarrow S + TiO_2 \quad (2.6)$$

Equation (2.5) and (2.6) are "parasitic" reactions that can reduce short circuit current,I_{sc} and lead to poor performance of DSSC.

The maximum theoretical value for the photovoltage (V_{oc}) depends on the potential difference between the redox potential and the Fermi level of TiO_2 at open circuit condition.

2.4 Photovoltaic parameters of DSSC

The sustainability of a DSSC is determined by its overall power conversion efficiency, stability and cost. The current-voltage (*I-V*) curve can determine the photovoltaic parameters of DSSC and are shown in Figure 2.3.

University of Malaya

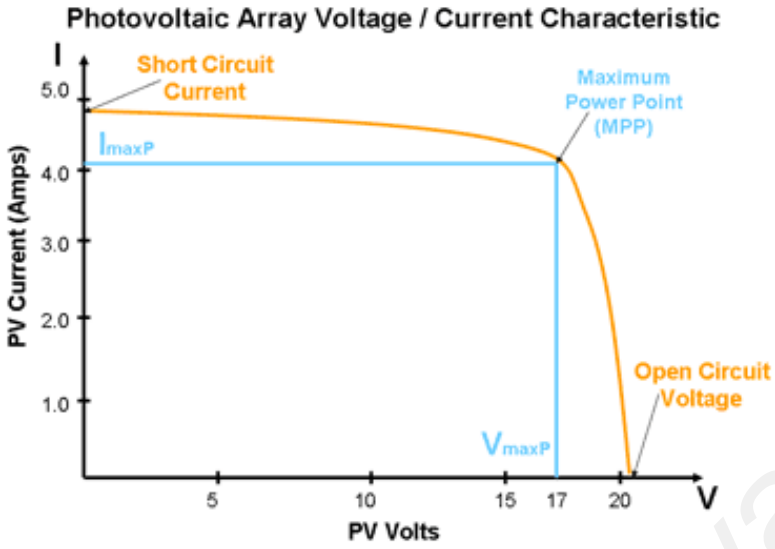

Figure 2.3. A typical current-voltage (I-V) curve of a DSSC.

The open-circuit voltage (V_{oc}) is the maximum voltage due to energy difference between the redox potential and the Fermi level of the semiconductor at zero current. In other words, when no current flows through the DSSC the maximum voltage is the open-circuit voltage,

$$V_{(\text{at } I=0)} = V_{oc} \tag{2.7}$$

The maximum current when the solar cell voltage is zero is short circuit current, I_{sc}. In other words,

$$I_{(\text{at } V=0)} = I_{sc} \tag{2.8}$$

Solar cell current is generally given as short circuit current density (J_{sc}), i.e.

$$J_{sc} = \frac{I_{sc}}{A} (\text{mA cm}^{-2}) \tag{2.9}$$

Here A is the active area, J_{sc} depends on solar irradiation, optical properties and charge transfer that occurs in the solar cell.

The power per unit area of the cell is the product of current density and the corresponding voltage on the *J-V* curve. The maximum power (P_{max}) is the product of maximum current density and voltage at the maximum power output ($P_{max} = J_{max} \times V_{max}$).

University of Malaya

FF is the ratio of the P_{max} to the product of V_{oc} and I_{sc}. The ratio of P_{max} to total intensity of photons (P_{in} = 100 mW cm^{-2}) gives the overall efficiency (η) of the solar cell.

$$FF = \frac{V_{\max} \times J_{\max}}{V_{\mathrm{oc}} \times J_{\mathrm{sc}}} \tag{2.10}$$

The solar cell efficiency (η) is the ratio of the maximum output electrical power P_{out} to the input power P_{in} according and is given by the equation.

$$\eta(\%) = \frac{V_{oc} \times J_{sc} \times FF}{P_{in}} \times 100 \tag{2.11}$$

Generally, efficiency is given in percentage.

Researchers use a solar simulator, which approximates the illumination of natural sunlight. A standardized measurement for P_{in} is the solar power of a 100 mW cm^{-2} for an air mass (AM) of 1.5.

The following sections discuss some basic aspects and considerable growth for each of the different DSSC components.

2.5 Components of DSSCs

The components of a DSSC are the conducting oxide glass plate, dye sensitizer, semiconducting oxide (e.g., TiO_2), counter electrode (CE) and the electrolytes. These are involved in the overall function of DSSC and is shown in Figure 2.4.

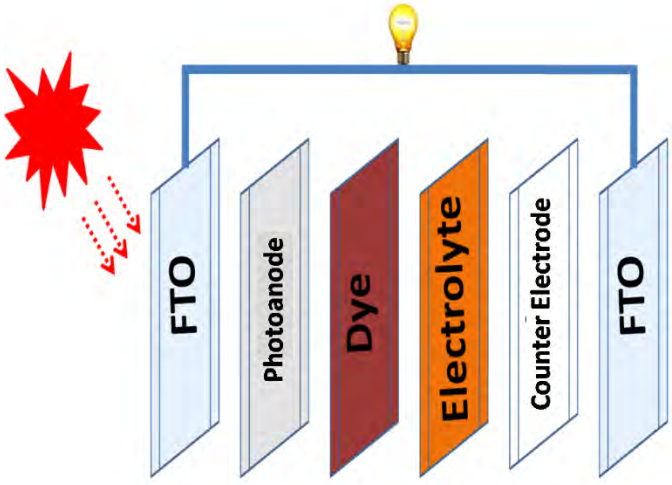

Figure 2.4. The major component of DSSC.

University of Malaya

2.6 Conducting glass substrates

The conducting glass substrate should be highly transparent to allow the higher penetration capacity of solar energy to the dye loaded area (active area). The properties of conducting plate also determine the solar cell efficiency as it should minimize the energy losses. There are two types of conducting oxide substrate used in DSSCs such as fluorine doped tin oxide substrate denoted by FTO and indium doped tin oxide substrate denoted by ITO. The transmittance of ITO films and FTO films in the visible region is about ~80 %, ~75 % with sheet resistance of 18 Ω cm^{-2}, 8.5 Ω cm^{-2} respectively (Mehmood *et al*., 2014). Sima *et al.* (2010) used both FTO and ITO glass substrates to fabricate the DSSCs and obtained the power conversion efficiency 9.4% and 2.4% respectively. This is may be due to the effect of sintering the glasses at 450 ^{o}C. The ITO sheet resistance increased from 18 to 52 Ω cm^{-2} but the FTO sheet resistance remained constant. Hence, FTO glass substrate is widely used in DSSC due to its conduction and stable sheet resistance at higher temperatures.

2.7 Photoanode: the TiO_2 layer

In DSSCs, one of the important parts is the porous semiconducting layer. It is prepared using porous semiconductor metal oxides like TiO_2 (Fukai *et al*., 2007), ZnO (Chou *et al.,* 2012), SiO_2 (Nguyen *et al.,* 2007), Nb_2O_5 (Cho *et al.,* 2013), AlO_3 (Kumara *et al.,* 2013) etc. The porosity largely enhances the surface area that allows more dye molecules to be loaded onto the semiconducting oxide layer and thus improves light absorption. Gorischer *et al.* (1960) fabricated the first dye sensitized photogalvanic cell using ZnO single crystal .The efficiency was less than 0.5 %. This is due to the smooth surface of the crystal that did not enable large dye loading, leading to insufficient light absorption.

University of Malaya

Gräetzel *et al*. (1991) assembled a nanocrystalline DSSC applying mesoporous TiO_2 and it showed the high efficiency of 7.5 %, which was a breakthrough in the development of DSSC research. The increase in efficiency is due to the increased surface area the TiO_2 that allowed a larger amount of dye molecule to be adsorbed on the TiO_2 layer. Among the metal oxides, TiO_2 is most popularly used in DSSCs due to its stability, low cost, availability, non-toxicity, biocompatibility and the better power conversion efficiency that can be achieved in the cell Gräetzel *et al*. (1991).

The TiO_2 coating is important in DSSC. This is because microstructure, particle size, porosity and pore size distribution on the photo anode affect the cell performance. There are several well established and inexpensive methods to coat the TiO_2 layer like as doctor blade, screen printing, electrophoretic deposition, spray coating and spin coating techniques which are used to make the TiO_2 porous film on the conducting glass plate for DSSCs.

2.8 Counter electrode

The main function of the counter electrode in DSSCs is to aid in completing electron flow circuit. The electron reduced I_3^- to I^- at the conducting substrate/electrolyte interface. To fulfil this requirement efficiently, the surface of counter electrode is activated using a suitable catalyst. There are several types of catalytic materials are used as counter electrode in DSSCs such as platinum (Kung *et al*., 2012) carbon based materials (Li *et al*., 2008), conducting polymers (Wu *et al*., 2008), and transition metal-containing materials (Gong *et al*., 2012) . Among these, Pt catalyst has high transparency, higher catalytic activity and high current exchange density (Fang *et al.,* 2004). The performance of the counter electrode depends on the methods of coating catalytic materials on conducting glass substrate (Wu *et al*., 2011). The following methods such as electrode deposition, sputtering, vapour deposition, screen printing, spin coating and drop

University of Malaya

casting techniques are used to deposit plastisol or platinum solution on the conducting glass substrate.

2.9 Liquid electrolytes

In DSSC, liquid electrolytes containing redox couples such as I^-/I_3^-, Co (III/II) and SCN^-/SCN_2 can be employed. The main function of the electrolyte is to access road the electric circuit by transporting positive charges to the counter electrode and regeneration of dye molecules after electron injection in to TiO_2. The stability of the DSSC is highly dependent on the properties of the electrolyte. Most of the DSSCs have been fabricated with liquid electrolytes. The highest light to electricity conversion efficiency of liquid electrolytes based DSSC achieved till now is 14% (Kakiage *et al.,* 2015). The main components of the liquid electrolytes are redox couple, organic solvent and additives. The following properties are necessary for a liquid electrolyte in DSSCs.

i. The redox potential should be more negative than the HOMO energy level of the dye.
ii. The redox species should have higher reducing capability to regenerate the dye.
iii. The electrolyte must have long-term stability.
iv. It should have low viscosity as well as high ionic conductivity.
v. The electrolyte should have good interfacial contact between photoanode and the counter electrode.
vi. It should not prevent dye adsorption on the TiO_2 surface.
vii. It should be stable up to ~80 ^oC.
viii. The electrolyte should not absorb light in the visible range.

University of Malaya

2.9.1 Organic solvent

The organic solvent is the essential component for I^-/I_3^- ions diffusion and dissolution in liquid electrolytes. In DSSCs organic solvents (Lee *et al*., 2009, Hara *et. al.*, 2001) used include acetonitrile (AcN), dimethylformamide (DMF), dimethyl sulfoxide (DMSO), propylene carbonate (PC), ethylene carbonate (EC), *N*-methyl-2-pyrolidone (NMP) and methanol. The physical properties of solvent e.g. viscosity, donor number and dielectric constant can affect performance of the DSSC (Bella *et al*., 2013). Among them, acetonitrile (AcN) is known to be the most efficient organic solvent for good solar cell efficiency (Lee et al., 2009). This may be due to its low viscosity and good solubility to dissolve salt and organic components in the electrolytes (Lee *et al*., 2009). *N, N*-Dimethylformamide (DMF) is well known effective solvent in DSSCs application (Lee *et al*., 2009). The physical properties of few organic solvent are listed in Table 2.1.

Table 2.1. Physical properties of some organic solvents

Solvent name	Boiling point (°C)	Melting point(°C)	Density (g/mol)	Viscosity(cP)	Dielectric constant
Acetonitrile(AcN)	81.65	- 43.8	0.7857	0.37 at 15 (°C)	35.9
N,N-Dimethyl formamide(DMF)	153	-60.4	0.9445	0.79 at 20 (°C)	36.1
Ethylene Carbonate(EC)	238	36	1.32	90.0 at 20 (°C)	90.0
Propylene Carbonate(PC)	241	-49	1.21	2.52 at 20 (°C)	65.0
Dimethyl sulfoxide(DMSO)	189	18.4	1.092	2.2 at 20 (°C)	46.5
Methanol	64.6	-98	0.791	0.545 at 20 (°C)	33
Ethanol	78.5	-114.1	0.789	1.08 at 25 (°C)	25
N-methyl-2-pyrolidone(NMP)	202	-24	1.033	1.7 at 25 (°C)	32

2.9.2 Redox couple

The redox couple plays an extremely significant role in DSSCs. The redox couple is obtained by mixing chemical species that have different oxidation states and can act as

University of Malaya

a reducing or oxidizing agent. Since the first development of DSSCs in 1991, the most widely used redox couple is I^-/I_3^-, because it is prepared by using iodide salts and iodine and showed a high power conversion efficiency. This can be obtained due to its stability to regenerate the dye and the relatively slow recombination losses through reaction with injected electrons which in turn increases electron concentration at the photoanode. Apart from this, $SCN^-/(SCN)_3^-$ (Oskam *et al*., 2001), Br^-/Br_3^- (Ferrere *et al.*, 1997), $SeCN^-/(SeCN)_3^-$ (Bella *et al.,* 2013), cobalt complexes (Mathew *et al*., 2014), sulphur-based systems (Liu *et al*., 2013), ferrocene derivatives (Daeneka *et al*., 2011) and stable nitroxide radical (Kato *et al.*, 2012) based redox couples are alternative mediators to the replace I^-/I_3^- redox couples. However, the alternative redox couples mentioned face problems that involved electron recombination, dye regeneration and slow reduction of oxidized species at the counter electrodes (Liu *et al*., 1998).

2.9.3 Additives

Additives are another crucial component in liquid electrolytes to improve photovoltaic performance of DSSCs. The additives are expected to be adsorbed onto TiO_2 surface and this can affect the position of the TiO_2 conduction band. This will determine the photocurrent and photovoltage of the DSSCs. The incorporation of additives into the electrolytes has been successful for important of V_{oc} and improving DSSC performances (Hara *et al.,* 2004). Nitrogen-containing heterocyclic compounds are the most widely used additives to prevent recombination reaction and improve the cell performance (Hara *et al.,* 2004). The addition of tert-butyl-pyridine (TBP) is able to reduce electron recombination at the TiO_2/electrolytes interface via the coordination N atom in TBP, with Ti ion, which helped to increase the V_{oc}, FF as well as efficiency of DSSCs (Hara *et al.,* (2004). Gräetzel *et al.* (1993) used TBP as additive in liquid electrolytes that resulted in significant improvement of the V_{oc}. The addition of TBP into the liquid electrolytes was

University of Malaya

studied by Boschloo *et al.* (2010) and it was found that increase in V_{oc} could be attributed to the combined influence of TiO_2 conduction band towards a negative direction and also to the longer electron life in the TiO_2 conduction band. Furthermore, Kusama *et al*. (2008) also studied the large number of nitrogen containing heterocyclic compounds such benzimidazole, aminotriazole, pyrimidine, aminothiazole, pyrazole and quinoline derivatives. This compounds also behaved in a similar way to TBP.

2.10 Polymer electrolytes in DSSCs

The fabricated DSSCs with 14% efficiency are based on liquid electrolytes (Kakiage *et al*., 2015). However, liquid electrolytes have certain problems such as being volatile, leakage and etc. Therefore, effects have been harnessed to replace the liquid electrolytes with solid or quasi-solid state polymer electrolytes (Shah *et al*., 2016). The solid state electrolytes can be ionic liquids entrapped in a polymer host and hole transport materials in polymers and polymer-salt complexes. Among these, polymer salt complexes are most preferred due to easy preparation, good stability and low cost. However, polymer complexes exhibits lower electrical conductivity compared liquid electrolytes. To enhance conductivity, plasticizers, ionic liquids and fillers have been added. Polymer blending has also been considered.

For solid-state DSSC applications, the following properties are requirements for good polymer electrolyte (Singh *et al*., 2011).

1. The polymer should have a flexible chain with a large number of polar groups (e.g. O, N, and S)
2. The polymer electrolyte should have high ionic conductivity.
3. It should have good thermal stability at temperatures ranging from -40 ^{o}C to 80 ^{o}C.
4. The polymer should have amorphous region to increase ionic conductivity.

University of Malaya

5. The polymer electrolyte should have a good chemical compatibility with anode and cathode.

2.11 Dye as sensitizer

Photo-sensitizing dye of DSSCs captures photons from the sun to generate electron flow or current. A good dye should has properties that enable the efficient conversion of light to electricity (Kuppuswamy & Grätzel, 2009). These are,

i. Light in the visible region of the electromagnetic spectrum (400-700 nm) must be absorbed intensively.
ii. Have strong anchoring attachment to the semiconductor. The photosensitizer should have the anchoring groups such as -COOH, -H_2PO_3, and -SO_3H which can help the photosensitizer to bind strongly onto the semiconductor.
iii. The dye's LUMO must be more negative higher than the conduction band edge of TiO_2.
iv. The sensitizer ground state should at a more positive level than the redox potential.
v. The adsorbed dye on the TiO_2 surface must be stable for a long cell life.
vi. The dye must show good solubility.
vii. The sensitizer should possess a high extinction coefficient.

Based on DSSCs application, many different photosensitizing materials such as porphyrins, phthalocyanines and metal-free organic dyes have been used in DSSCs.

2.11.1 Ruthenium (Ru) dye

Ru-centered polypyridyl complexes such N3 and N719 have resulted in power conversion efficiency of more than 11% and this is due to their good optical and electronic properties like a broad absorption spectra, suitable energy band gap and good chemical stability (Kuppuswamy & Grätzel, 2009). Although metal based sensitizers has produced

University of Malaya

a higher efficiency but these precious metals is expensive and environmental unfriendly. The structure of some of high performance Ru-metal based dye molecules with their efficiencies are shown in Figure 2.5.

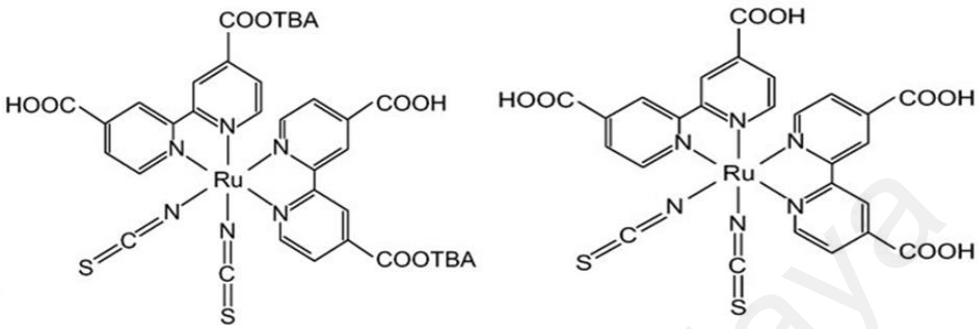

N719 Dye (η=11.1 %) N3 Dye (η=10 %)

Figure 2.5. The structure of some of high performance Ru-metal based dye molecules with their efficiencies (Nazzeruddin *et al.,* 1993).

2.11.2 Organic dyes

Compared to noble metal complexes, organic dyes are cheaper and environmental friendly. Organic dye has donor acceptor (D-π-A) structure which make them as alternative to Ru complexes. On absorption of light, charge transfer occurs within the molecule from acceptor to donor via the π-bridge. Organic dyes have been modified to improve DSSC performance. Many n-type organic dyes (Mishra *et al.,* 2009 and Ooyama *et al*., 2009), coumarin dyes (Hara *et al*., 2001 and Hara *et al.,* 2003), indoline dyes (Dentani *et al.,* 2009), carbazole dyes (Wang *et al.,* 2008), hemicyanine dyes (Wang *et al.,* 2000), merocyanine dye (Sayama *et al*., 2000), perylene dyes (Li *et al.,* 2007), anthraquinone dyes (Erten-Ela *et al*., 2008), and polymeric dyes (Liu *et al.,* 2008) have been used as sensitizers for DSSCs. Donor-*p*-Acceptor structure principle of an organic dye in DSSCs with TiO_2 photoanodes are shown in Figure 2.6.

University of Malaya

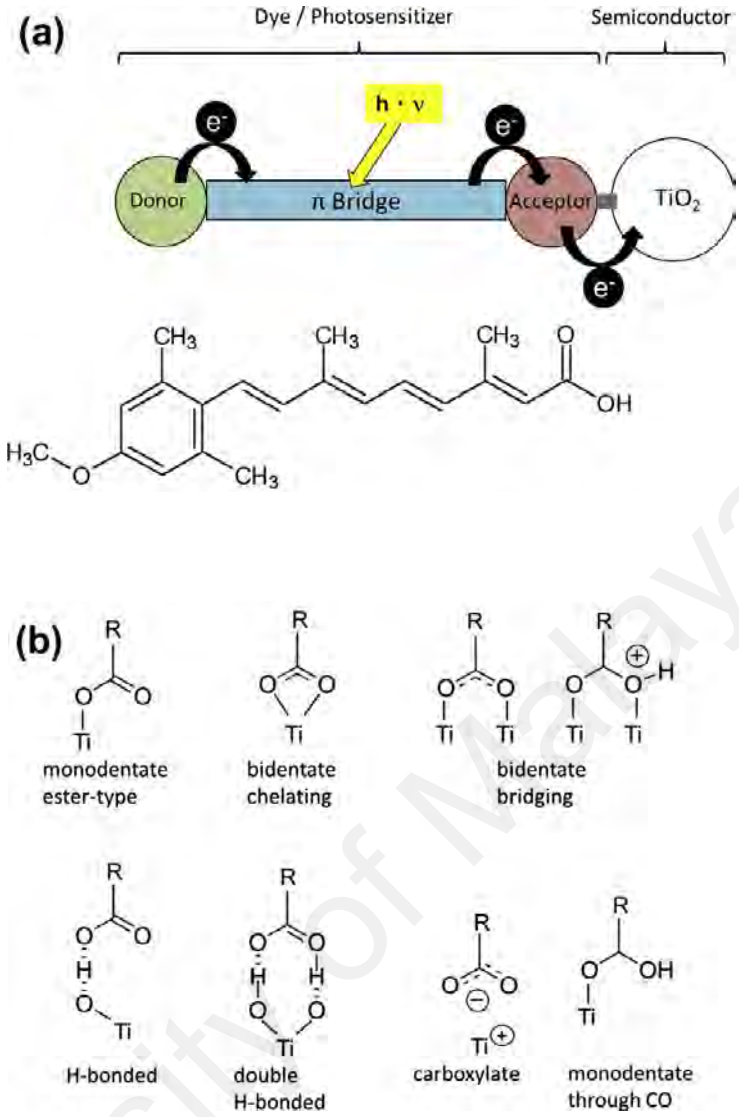

Figure 2.6. (a) Donor-p-acceptor structure principle of an organic dye in DSSCs with TiO2 photoanodes (Nazzeruddin *et al.,* 1993), (b) Possible binding modes of a COOH-group to TiO_2. (Pan *et al*., 2002)

2.11.3 Natural dye sensitizers

In nature plenty of colourful pigments that can be readily extracted and used for DSSC fabrication (Chang and Lo, 2010). These pigments have been considered as promising alternative sensitizers for DSSCs due to their low cost, simple preparation technique, biodegradability, availability, and most importantly reduction on the use metal based sensitizer (Keka *et al.,* 2012).

The performance of natural sensitizers in DSSC has been evaluated by the equation of energy conversion efficiency (η). Several pigments have been the popular

University of Malaya

subject of research e.g. chlorophyll (Kumara *et al*., 2006, Hao *et al.,* 2006), carotenoid (Gomez-Ortiz *et al.,* 2010), anthocyanin (Alhamed *et al.,* 2012, Chang and Lo, 2010), flavonoid (Keka *et al.,* 2012), cyanine (Furukawa *et al.,* 2009), and tannin (Kamel *et al.,* 2005). Natural colorants are pigmentary molecules obtained mainly from plants with or without chemical treatments. Natural colorants have a hydroxyl groups in their structure to bind with semiconductor (Alhamed *et al.,* 2012). So it gives low efficiency in application of DSSCs with natural sensitizers. Several colorants do not have solubilizing group; hence, a temporary solubility group is generated during application (Furukawa *et al.,* 2009). The chemical structure of some natural sensitizers are shown in Table 2.2.

Table 2.2 Some chemical structure of the natural dyes (Furukawa *et al* 2009)

Name	**Chemical structure**
Bixin	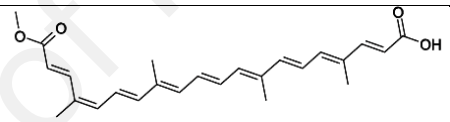
Crocetin	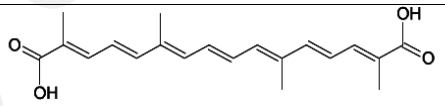
Crocin	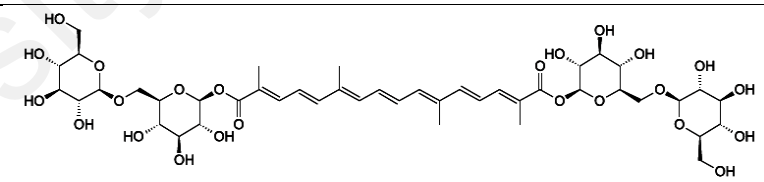
Betaxanithin	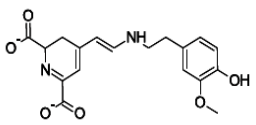
Betalains	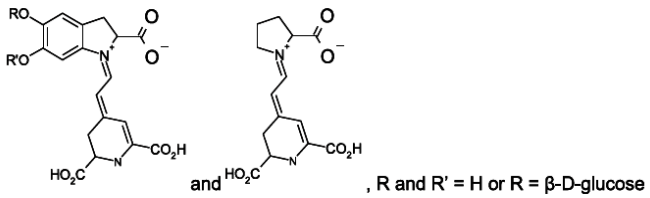
Delphinidin (an anthocyanidin)	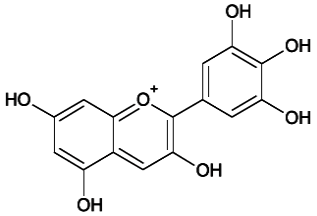

University of Malaya

Table 2.2, continued…

Cyanidin (an anthocyanidin)	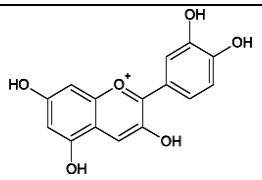
Cyanin (an anthocyanin)	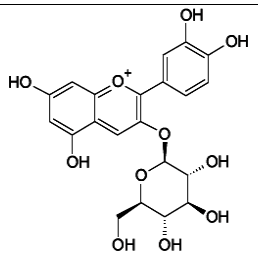
Nasunin (an anthocyanin)	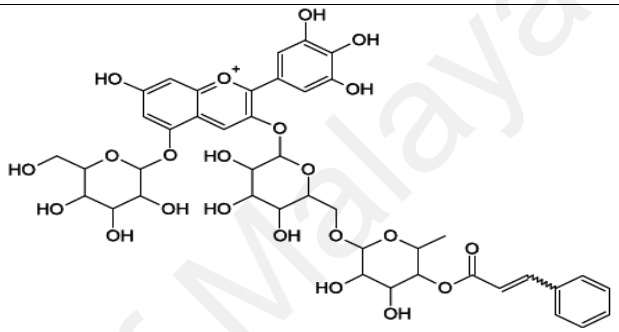
Peonidin (an anthocyanidin)	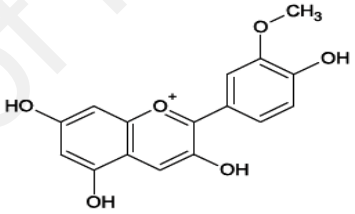
α-Mangostin	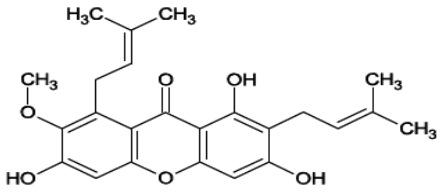
β-Mangostin	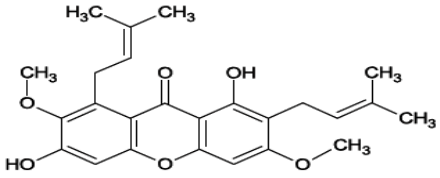
Chlorophyll a	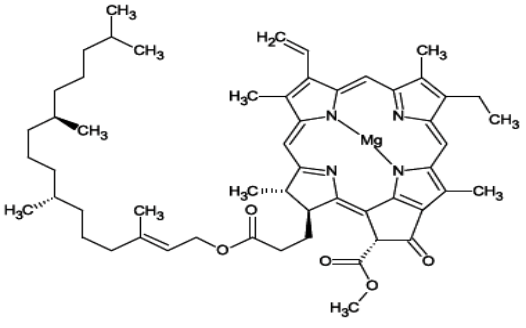

University of Malaya

Table 2.2, continued…

Rutin (a flavonol glycoside)	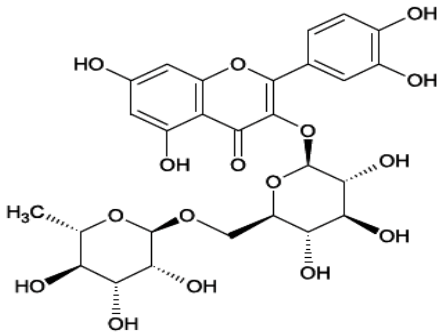
Methyl-3-carboxy-3-devinylpyropheophorbide (a modified chlorophyll)	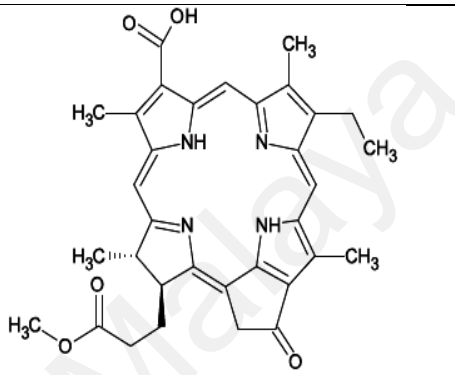
Neoxanthin	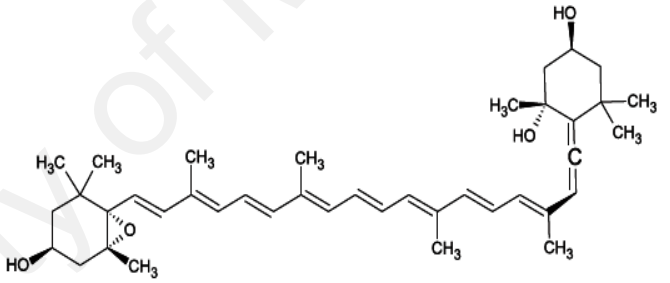
Violaxanthin	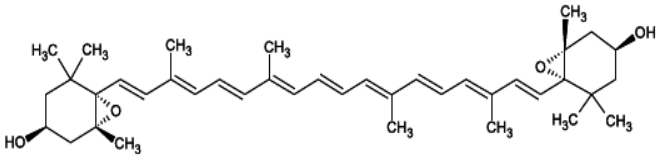
Lutein	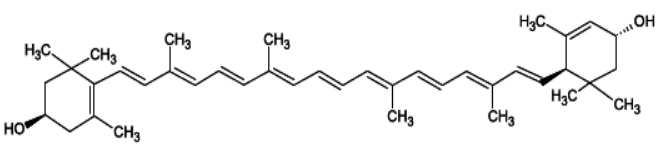
β-Carotene	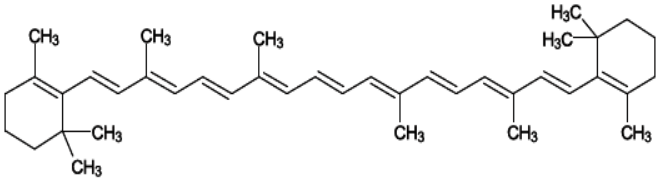

University of Malaya

2.11.4 Flavonoid

Flavonoid is the term that describes a great collection of natural pigments which includes a phenylbenzopyran functionality (Grotewold, 2006). The degree of phenyl ring oxidation (C-ring) identifies the different colors of flavonoids. However, they all have similar structures but all flavonoids do not have the same light absorption capacity. Flavonoid molecules are characterized by loose electrons; thus, the energy required for electron excitation to LUMO is lowered, allowing pigment molecules to be energized by the visible light. The various flavonoid pigment colours are determined by the wavelengths of the visible light absorbed by pigment molecules and those that are reflected. The adsorption of flavonoid to the mesoporous TiO_2 surface is fast, displacing an OH counter ion from the Ti sites that combines with a proton donated by the flavonoid structure (Narayan and Raturi, 2011). Over 5000 naturally occurring flavonoids have been extracted from various plants, and are divided according to their chemical structure as follows: flavonols, flavones, flavanones, isoflavones, catechins, anthocyanin, and chalcones. Anthocyanin belongs to a natural group that provides colour to the flowers, fruits and leaves of plants, and it has also absorption in the purple-red region (Polo *et al*., 2006).

Anthocyanin can also be found in roots, tubers, and stems of the plant organs (Patrocinio *et al.,* 2009), and are widely distributed in plant seeds. The molecular structure of anthocyanin is shown in the chemical structure of Table 2.2. Anthocyanin molecule have binding groups (carbonyl and hydroxyl) that can bind to the semiconductor TiO_2 surface. This helps electron transfer from sensitizer to the TiO_2 conduction band upon photon illumination (Hao *et al.,* 2006). Anthocyanin extracted from different plants provides various sensitizing performances (Luo *et al.,* 2009).

Nishantha *et al*. (2012) used an anthocyanin dye extracted from the barks of *Kopsia flavida* fruit that showed J_{sc} = 1.2 mA cm^{-2}, V_{oc} = 520 mV, and FF = 0.62. Wongcharee

University of Malaya

et al., (2007) extracted anthocyanin-rich natural dyes from the flowers of rosella and blue pea as sensitizers for DSSC. They have investigated the performance of the DSSC using mixed blue pea–rosella dye and hypothesized that two anthocyanin dyes having various absorption spectrums than the single dye.

2.11.5 Carotenoid

Carotenoids, anthocyanin and flavonoids are organic pigments that naturally occurs in the same organs of plants. Carotenoid pigments are usually responsible for yellow to orange petal colours (Teresita *et al.,* 2010). Carotenoids are light-harvesting pigments and have important roles in photosynthesis protection. Carotenoids pigments complement chlorophylls through redox reactions. The pristine natural pigments perform better than their purified counterparts (Koyama *et al*., 2012). This is due to alcohols and organic acids present. This compounds assist dye adsorption, prevent electrolyte recombination, and decrease dye accumulation. Hemalatha *et al*. (2012, reported that *Kerria japonica* carotenoid dye sensitizer has conversion efficiency is 0.22 %. Carotenoids are compounds consisting of eight isoprenoid units that are widespread in nature, and have great potential as energy harvesters and sensitizers for DSSCs (Hemalatha *et al.,* 2012).

Theoretical evaluation of the chemical and physical properties of natural dye as sensitizers are important in establishing performance and structure properties of dyes sensitizers (Zhang *et al*., 2009). Koyama *et al*., (2012) reported that the main factor for the increased cell performance is the reduced interaction among the excited state dye sensitizers. Some carotenoic acid and retinoic-acid sensitizers also contain n-conjugated double bonds (Zhang *et al.,* 2009). Yamazaki *et al*. (2007) studied crocetin, and crocin as sensitizers. The efficiency of crocetin-sensitized DSSCs (0.56%) is three times, or higher than crocin (0.16 %), because of the presence of carboxylic groups in the crocetin molecule (Yamazaki *et al*., 2007).

University of Malaya

2.11.6 Chlorophyll

Chlorophyll (Chl) is found in the leaves of most green plants, algae, bryophytes and also in cyanobacteria (Hassan *et al*., 2014). The most occurring type is Chl a. There are six different types of Chl pigments exist in nature. The molecular structure of chlorophyll is formed by a magnesium (Mg) ion.

Chl are the principal pigments in natural photosynthesis systems (Chang *et al*., 2011). Chl include a group of more than 50 tetrapyrrolic pigments. Chl and their derivatives are inserted into DSSC as dye sensitizers because of their beneficial light absorption tendency modes; the most efficient of which is Chl a (chlorine 2) derivative-methyl trans-3^2-carboxy-pyropheophorbide α. Wang *et al*. (2010) reported that chlorine 2 has an ability to anchor onto TiO_2 and ZnO semiconductors surfaces through different modes. Chl has an absorption peak at 670 nm. Amao and Komori (2004) reported that the chlorine-e_6 created by Chl hydrolysis contains three carboxylate groups per molecule. The absorption spectrum of Chl-e_6 is similar to that of Chl. The J_{sc}, V_{oc} and *FF* of the solar energy cell using Chl-e_6 are 0.31 $mAcm^{-2}$, 0.43 V, and 0.45, respectively (Amao and Komori, 2004).

2.12 The dye anchoring on the TiO_2 semiconductor

Generally, there are six different ways how a molecular can be adsorbed on a surface. These are classified as follows: (a) covalent attachment brought about directly by linking groups of interest or via linking agents, (b) electrostatic interactions, brought about via ion exchange, ion-pairing or donor-acceptor interactions, (c) hydrogen bonding, (d) hydrophobic interactions leading to self-assembly of long chain fatty acid derivatives, (e) van der Waals forces involved in physisorption of molecules on solid surfaces, and (f) physical entrapment inside the pores or cavities of hosts such as cyclodextrins, micelles, etc. (Kalyanasundaram and Gra”tzel 1998). Dye adsorption on semiconductor surfaces

University of Malaya

depends on dye-semiconductor strong interlinkage. Thus the dye requires an anchoring group to form attachment with the semiconductor surface. There are number of anchoring groups such as carboxylic (-COOH), ester, acid chloride, acetic anhydride, sulfonate ($-SO_3^-$) and silane (SiX_3) or $Si(OX)_3$.

Most photosensitizers have carboxylic acid anchoring group. This is due to its relative stability and easy synthesis. However, there are different ways of binding between the carboxylic acid and the semiconducting oxide surface which are shown in Figure 2.7 (Deacon and Phillips, 1980).

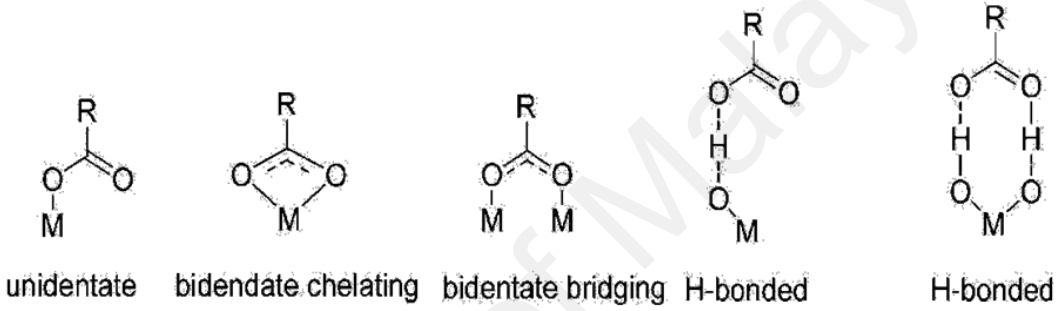

Figure 2.7. Binding modes for carboxylate unit on TiO_2 surface (Deacon and Phillips, 1980).

2.13 Combining sensitizers

In order to extend adsorption on the mesoporous TiO_2 surface, many approaches have been developed e.g. incorporation of a mixed dye sensitizer. Spitler *et al.* (2001) have combined cyanine dyes in DSSCs and compared to the performance of DSSCs with single dyes. Ozawa and Arakawa (2012) reported an 11% efficiency by mixing a Ru complex and an organic sensitizer (D131). Clifford *et al*. (2004) developed a method of double layer dye adsorption photoanode. Using this co-sensitization method and combining two organic dyes, Choi *et al*. (2008) and Chiron *et al*. (2014) also obtained very high efficiency in DSSCs.

University of Malaya

2.14 Summary

Inorganic solid-state junction Si devices is being challenged by the emergence of DSSCs. Among the basic components of DSSCs, sensitizer are the main effective component. The metal based ruthenium dye has been showing the highest cell efficiency compare to other types of dye sensitized solar cell. But due to their some disadvantages, alternative sensitizer need to find for DSSC application. The use of natural dyes as sensitizers in DSSCs provided an alternative source because they are cheap, eco-friendly, available in abundance and manufacture and use. Recent developments on different kinds of sensitizers for DSSC devices have led to the use of natural dyes that absorb sunlight within the visible spectrum providing higher efficiencies. The nature of the dye used as sensitizers is also the main factor affecting the DSSC efficiency. Although the stability and efficiency of this type of cells are still insufficient, they are expected to evolve soon because of the significant research efforts in developing all parts of the cell, especially, the sensitizers. The results of these studies encourage further research on the use of natural dye sensitizers to increase the ability of converting photon to electricity and stabilize DSSC for commercialization.

University of Malaya

CHAPTER 3: EXPERIMENTAL METHODS

3.1 Introduction

In the present work, black rice (anthocyanin) and fragrant screwpine (*Pandanus amaryllifolius*) chlorophyll were used as sensitizer for DSSCs. The TiO_2 electrode was dipped into each dye solution one after another using different combinations of dipping times. Ruthenium metal based dye sensitizer (N3) has also been used. Gel polymer electrolytes (GPE) consisting of phthaloylchitosan (PhCh), polyethylene oxide (PEO), dimethylformamide (DMF), ethylene carbonate (EC), tetrapropylammonium iodide (TPAI), iodine (I_2), tertbutyl pyridine (TBP) have been prepared for the fabrication of DSSCs. The optimized GPE has been added with TBP as additive and has been tested in DSSC. The photocurrent density-voltage (*J-V*) characteristic of DSSCs have been measured under white light illumination of 100 W cm^{-2} with active area 0.20 cm^2. The incident photon to current conversion efficiency (IPCE) was also characterized for the fabricated DSSCs. Electrochemical impedance spectroscopy (EIS) has been taken to investigate internal resistance of every solar cell.

3.2 Materials

Materials purchased were polyethylene oxide (PEO), tetrapropylammonium iodide (TPAI), ethylene carbonate (EC) and triton-X surfactant (Sigma-Aldrich), dimethylformamide (DMF) (Friedemann Schmidt Chemical) and iodine (I_2) crystals (Amcochemie-Humburg). Phthaloylchitosan was obtained by reacting of chitosan with phthalic anhydride (Merck-Germany). 15 nm (P90) and 21 nm (P25) TiO_2 particles were purchased from Evonik Industries. Polyethylene glycol (PEG) was purchased from Supelco, USA and methanol from John Kollin Corporation. Tetrapropylammonium

University of Malaya

iodide (TPAI) and tertbutyl pyridine (TBP) were purchased from Sigma-Aldrich. Platinum (plastisol) purchased from Solaronix.

3.3 Electrode Preparation

3.3.1 Glass substrate washing process

At first, the fluorine-doped tin oxide (FTO) glass substrate was cleaned with liquid soap and upright with distilled water, and then rinsed again with acetone. Secondly, the glass substrate was dried at room temperature and boiled in 2-propanol until bubbles shown to remove rest of dirt. The unstained FTO glass was then kept for further use.

3.3.2 TiO_2 photoelectrode preparation

The first TiO_2 layer or the compact layer was prepared by mixing 0.5 g of P90 powder with 2 mL of 0.1 mol nitric acid. The mixture was ground for 15 min. The TiO_2 paste was spin coated on the FTO substrate and heated at 450°C for 30 min. The second TiO_2 layer or porous layer was prepared by grinding 0.5g P25 powder and nitric acid of the same amount with 0.1 g PEG and few drops of surfactant. The doctor blade method was used to coat the porous layer above the compact layer and was then heated at 450°C for 30 min.

3.4 Dye solution preparation

Natural dyes (anthocyanin and chlorophyll) were extracted using very simple procedure. 200 g pandanus leaves were cut in many small pieces and washed with distilled water and leave it to dry. After that leaves are soaked in same amount of methanol (200 ml at pH = 1) solution to extract dye after 24 h. Extracted dye was filtered by filter paper and kept in fridge for further use. 200 g black rice was put in same amount of methanol to extract anthocyanin dye. After 24 h, the dye was extracted and filtered with filter paper.

University of Malaya

In addition, 3×10^{-4} M of ruthenium dye (N3) dye was prepared by immersing the dye in ethanol solution for 24 h, then the dye sensitized TiO_2 electrodes were washed with absolute ethanol and dried in air before assembling the DSSCs.

3.5 Counter electrode preparation

The plastisol solution is a paste containing platinum precursor which forms a quasi-invisible catalytic layer of platinum by heat treatment. The plastisol was added drop by drop on cleaned FTO glass until the surface turned opaque. The FTO glass was then heated at 450 ºC for 45 minutes.

3.6 Preparation of gel polymer electrolytes

A modified chitosan (phthaloylchitosan) was blended with polyethylene oxide (PEO) to prepare gel polymer electrolytes. The dimethylformamide (DMF) organic solvent was mixed with blended polymers at 80°C. The solution was stirred until it dissolved completely. Followed by this ethylene carbonate (EC) was added to increase amorphousness of polymer. Tetrapropylammonium iodide salt added to the solution and stirred until all compound dissolved properly. After the sample was cooled down at room temperature, crystals iodine were added in to gel polymer solution to form redox couple. For second polymer electrolytes system different weight percentage of tertbutyl pyridine (TBP) additive was added into polymer electrolytes. All the electrolytes composition are shown in Table 3.1 to Table 3.3.

University of Malaya

Table 3.1: Electrolytes composition for first system and its designation

Electrolyte	GPE1A		GPE1B		GPE1C		GPE1D	
	Gram (g)	wt.%	Gram (g)	wt.%	Gram (g)	wt.%	Gram (g)	wt.%
PhCh	0.08	5.11	0.08	5.04	0.08	4.97	0.08	4.91
PEO	0.02	1.28	0.02	1.26	0.02	1.24	0.02	1.23
EC	0.50	31.93	0.50	31.50	0.50	31.08	0.50	30.67
DMF	0.60	38.32	0.60	37.80	0.60	37.30	0.60	36.81
TPAI	0.34	21.71	0.36	22.68	0.38	23.62	0.40	24.53
I_2	0.0255	1.63	0.0270	1.70	0.0285	1.77	0.030	1.84

Table 3.2: Electrolytes composition (in gram) for second system and its designation.

Electrolyte	Conductivity, σ (mS cm^{-1})	PEO (g)	PhCh (g)	DMF (g)	EC (g)	TPAI (g)	I_2 (g)	TBP (g)
GPE 2A	10.72	0.02	0.08	0.5	0.6	0.36	0.027	0.032
GPE 2B	10.34	0.02	0.08	0.5	0.6	0.36	0.027	0.066
GPE 2C	10.13	0.02	0.08	0.5	0.6	0.36	0.027	0.101
GPE 2D	10.28	0.02	0.08	0.5	0.6	0.36	0.027	0.138
GPE 2E	10.37	0.02	0.08	0.5	0.6	0.36	0.027	0.177
GPE 2F	10.66	0.02	0.08	0.5	0.6	0.36	0.027	0.209

Table.3.3: Electrolytes composition (in wt.%) for second system and its designation

Electrolyte	PEO (wt. %)	PhCh (wt. %)	DMF (wt. %)	EC (wt. %)	TPAI (wt. %)	I_2 (wt. %)	TBP (wt. %)
GPE 2A	1.23	4.94	30.87	37.05	22.23	1.67	1.99
GPE 2B	1.21	4.84	30.24	36.29	21.77	1.63	4.00
GPE 2C	1.18	4.73	29.61	35.54	21.32	1.60	6.00
GPE 2D	1.16	4.64	28.98	34.77	20.87	1.56	8.01
GPE 2C	1.13	4.53	28.35	34.02	20.41	1.53	10.01
GPE 2E	1.10	4.43	27.72	33.27	19.96	1.5	12.00

3.7 Fabrication of DSSCs

The DSSC was assembled by sandwiching the photoanode and counter electrode. In between of photoanode and counter electrode, gel polymer electrolyte was used to give ionic conduction. The DSSC configuration was FTO/TiO_2-dyes/GPE/Pt/FTO and the fabricated DSSC images are shown in Figure 3.1. The *J-V* characteristics were measured with an auto lab electrometer under 1 Sun illumination. The solar cell active area was used approximately 0.2 cm^2.

University of Malaya

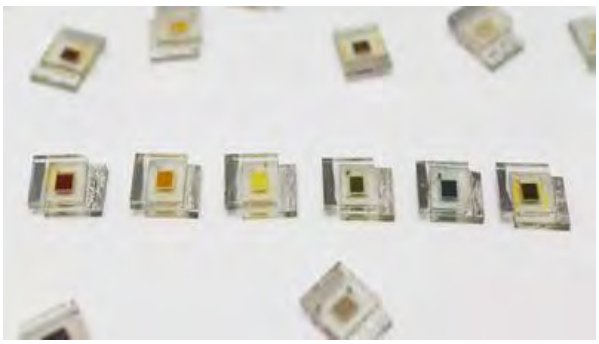

Figure 3.1. Image of fabricated DSSCs.

3.8 Characterization Techniques

3.8.1 UV-Vis Spectroscopy

The dyes were placed horizontally to spectrum line and its spectrum was taken using the UV-3101PC Shimadzu ultraviolet visible–near infrared (UVVIS-NIR) scanning spectrophotometer. The absorbance were measured from 400 nm to 750 nm.

3.8.2 Electrochemical impedance spectroscopy (EIS)

In this work, EIS was carried out to determine the ionic conductivity of polymer electrolytes and resistance of DSSC devices. Ionic conductivity of polymer electrolytes was measured using HIOKI 3532-50 LCR from the frequency range of 50 Hz to 5 MHz with the a.c voltage of 10 mV. The GPE were placed in a coin cell of 0.285 cm thickness and 2.271 cm^2 stainless steel electrodes surface area. The point of intersection of the impedance plot of the real axis gives the bulk resistance (R_b) of the sample, thus conductivity (σ) of a given sample may be expressed as

$$\sigma = t/R_b A \qquad (3.1)$$

where t is the thickness of the thin film, A the area of cross–section and R_b the bulk resistance of the sample.

The model of Nyquist plot (Figure 3.2 a) displays $-Z''$ against Z'. It is the most frequently used in electrochemical literature as it allows an easier prediction of the

University of Malaya

equivalent electronic circuit. However, it does not represent the frequency dependence and therefore it is complemented by the Bode plot.

The Bode plots (Figure 3.2 b and c) display the impedance or phase angle against the frequency which allows the determination of the absolute value of the impedance $|Z|$ and the phase shift φ.

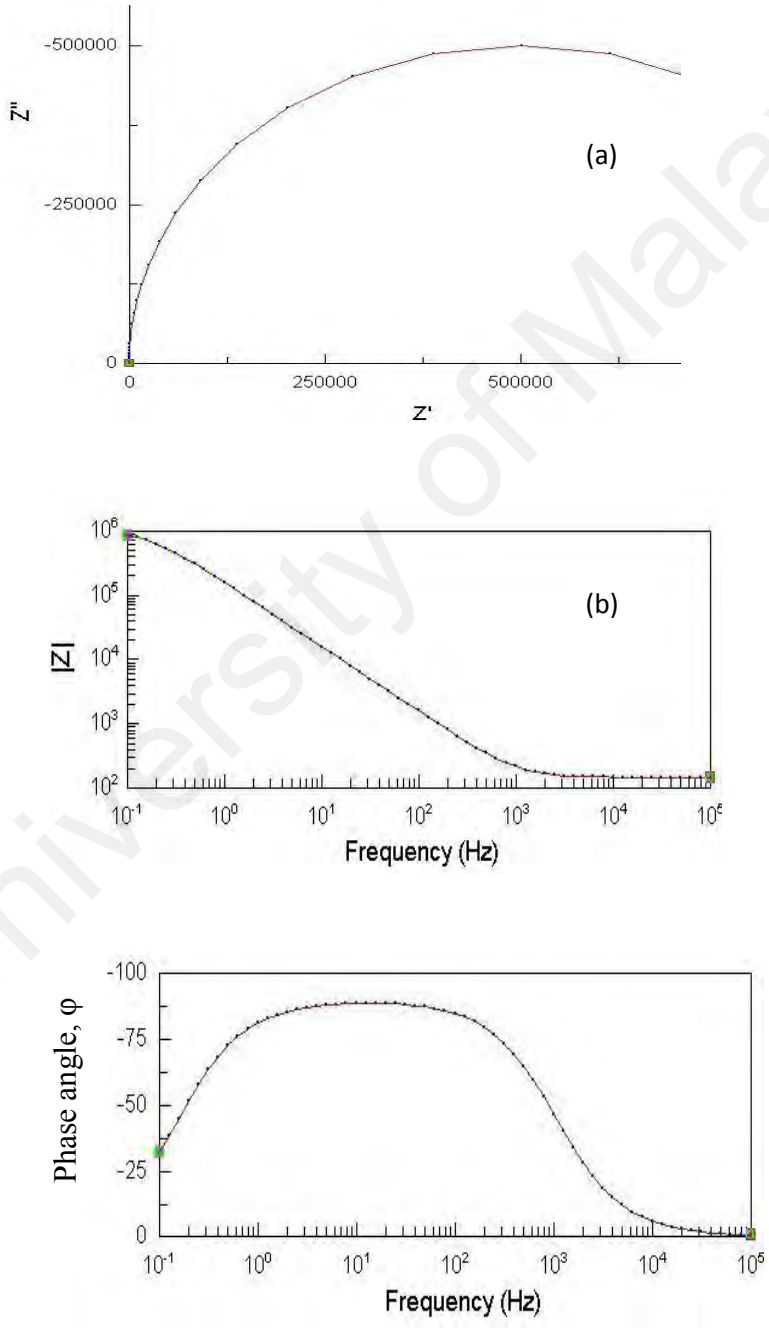

Figure 3.2 (a) Nyquist plot, imaginary part of the impedance, *Z''*, versus its real part, *Z'*, (b) Bode plot, absolute value of the impedance, $|Z|$, versus the frequency, and (c) Bode plot, phase angle, φ, versus the frequency.

University of Malaya

The internal resistance of DSSCs fabricated were carried out with an AUT 85988 advanced electrochemical system (Metrohm Autolab B.V. PGSTAT 128N Netherlands) from 1 mHz to 1 MHz at room temperature. All the measurements were carried out with applied bias of open circuit voltage (V_{oc}) under AM 1.5 global illuminations.

3.8.3 Incident photon-to-current efficiency (IPCE)

The incident photon-to-current efficiency (IPCE) was measured in the wavelength range from 300 nm to 900 nm using Newport Oriel setup. The measurements of IPCE are the measure of the ratio of total amount of incident photon that converted into the rate of photocurrent. Some incident photons are also converted into heat.

3.9 Summary

As a summary, the DSSC should consist of a photoanode, electrolyte with redox mediator and a counter electrode. The procedures for making each component and the characterization techniques have been presented in this chapter and will be used to obtain the results of the present study.

University of Malaya

CHAPTER 4: Results and Discussion (PhCh-PEO-DMF-EC-TPAI-I_2)

4.1 Introduction

In this work, different concentration of TPAI salt in wt. % were used to prepare gel polymer electrolytes. Conductivity measurement has been taken for all gel polymer electrolytes.

The prepared gel polymer electrolytes were used to fabricate the DSSCs. The DSSCs have been assembled with a ruthenium based dye as sensitizer. Besides this, natural pigment dyes have also been utilized to compare with synthetic dye on DSSCs. The *J-V* characteristics and IPCE of the DSSCs were measured using the Newport Model 70528 Oriel Monochromator Illuminator. The EIS measurement has also taken to investigate cell resistance.

4.2 The electrical conductivity of PhCh-PEO-DMF-EC-TPAI-I_2 electrolytes

Figure 4.1 shows the Nyquist plots at room temperature for the PhCh-PEO-DMF-EC-TPAI-I_2 GPEs. It can be observed in Figure 4.1 that the bulk resistance, R_b decreases with increasing salt concentration which indicates that the resistance of the movable ions decreases and leads to increase in ionic conductivity. The ionic conductivity increase up to 11.80 mS cm^{-1} for 22.68 wt. % of TPAI (GPE 1B). The increase in conductivity may be due to the increasing in number density and ion mobility. Moreover, from 23.62 wt. % to 24.53 wt. % of TPAI salt content, the R_b of the GPE increases and thus the conductivity is decreased. This is probably due to the formation of ion aggregation and decrease in ion mobility. Dissanayake *et al*. (2012) have studied gel polymer electrolyte using polyacrylonitrile (PAN), ethylene carbonate (EC), propylene carbonate (PC), TPAI and I_2. The highest ionic conductivity obtained was 2.4 mS cm^{-1} which is lower than the conductivity of GPE 1B.

University of Malaya

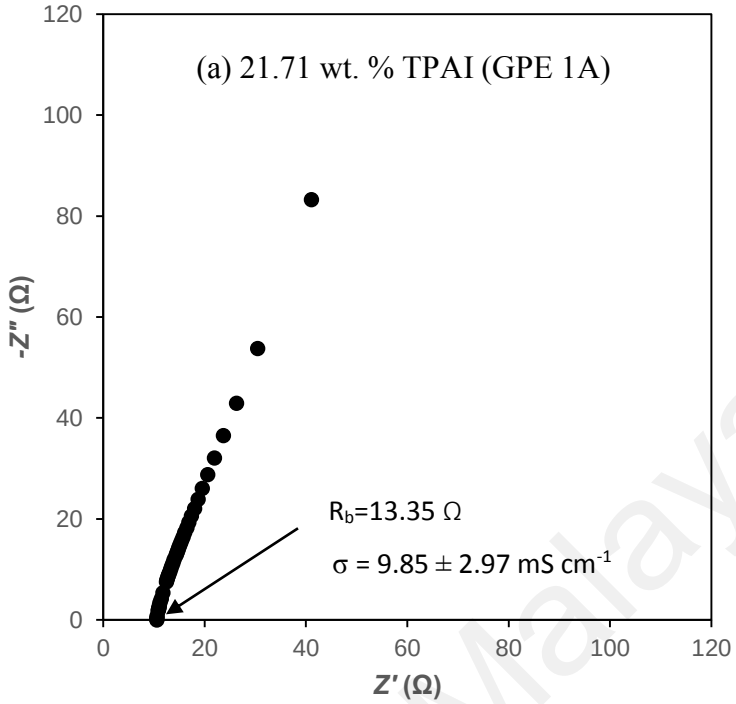

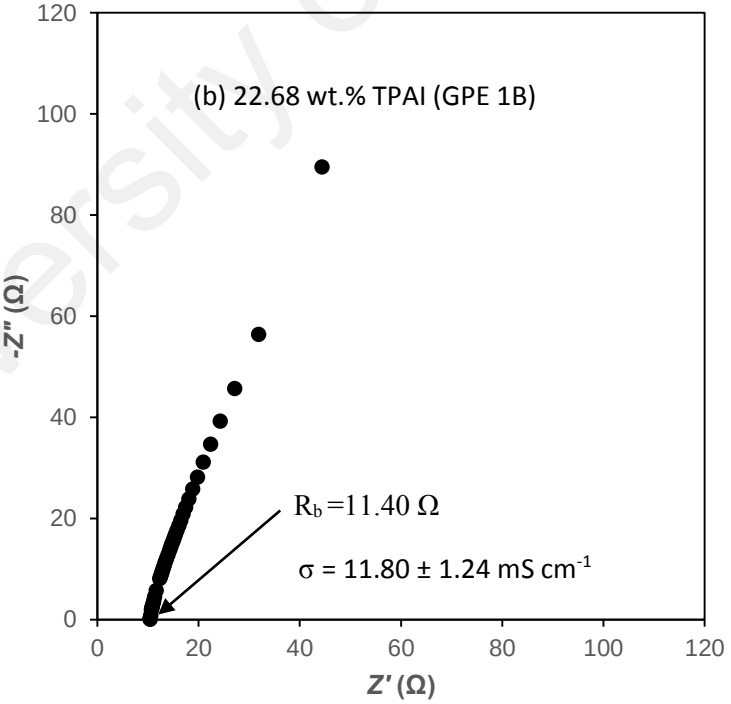

University of Malaya

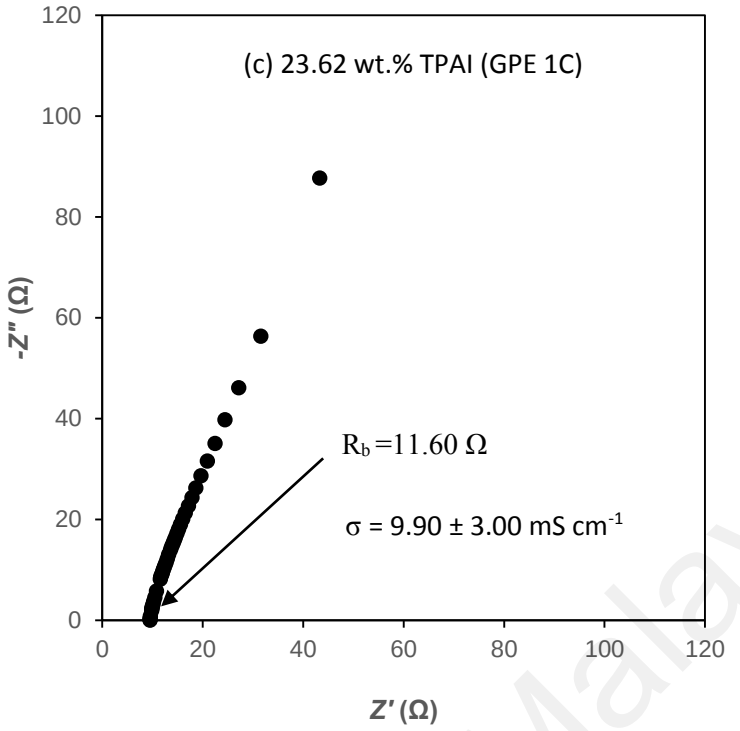

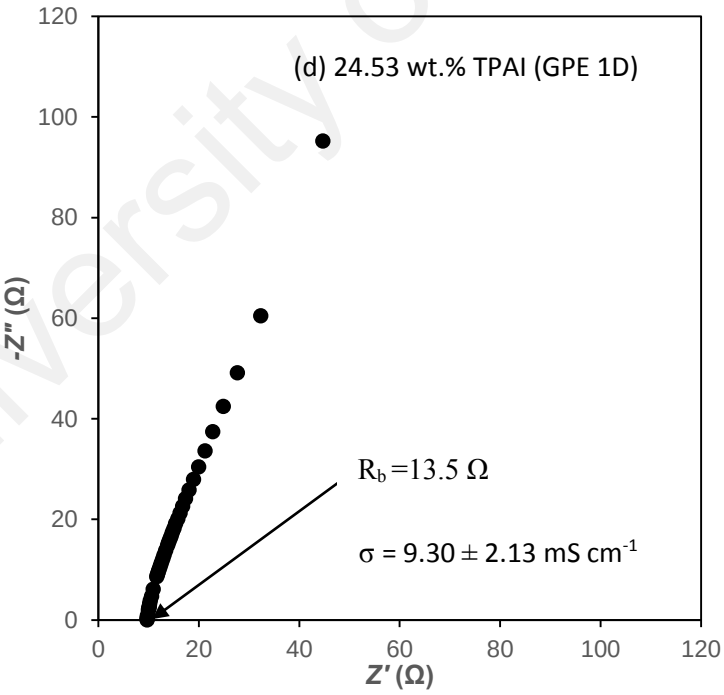

Figure 4.1. Nyquist plots of PhCh-PEO-DMF-EC-TPAI-I_2 GPE.

University of Malaya

Figure 4.2 shows the Log σ versus 1000/T for the GPEs. It is obvious that the conductivity for each GPEs increases with increasing temperature. This can be attributed to the increase in ions mobility and decreased in crystallinity of polymer matrix.

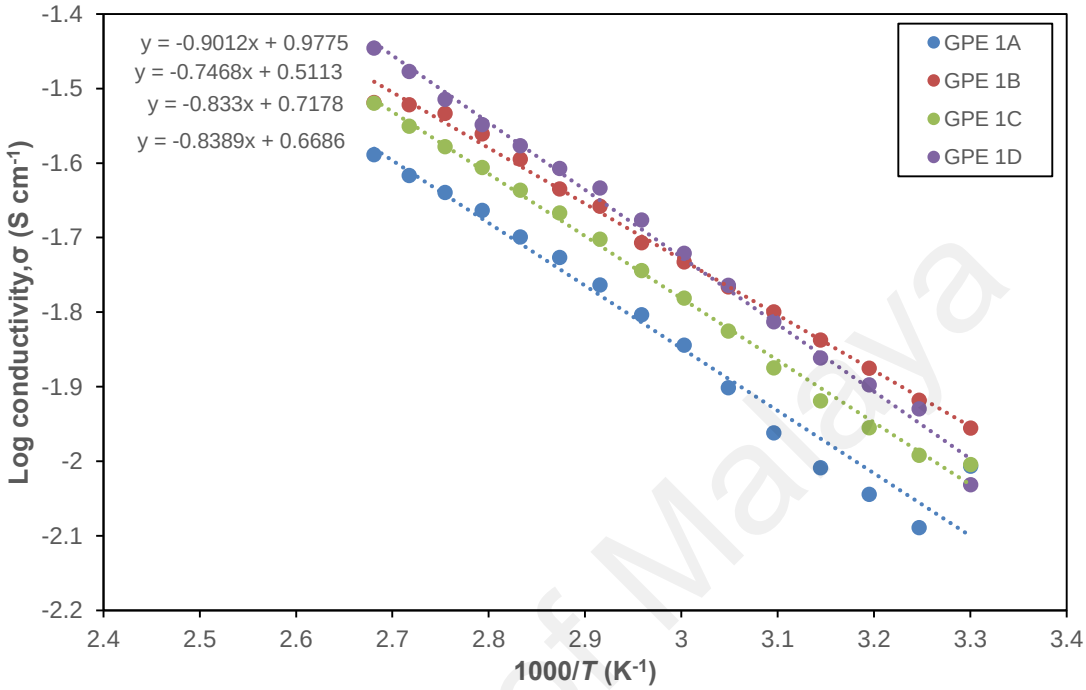

Figure 4.2. Conductivity-temperature dependence of gel polymer electrolytes.

The temperature dependence ionic conductivity for all GPEs shown in Figure 4.2 follow the Arrhenius relation;

$$\sigma = \sigma_0 e^{\frac{-E_A}{kT}} \qquad (4.1)$$

Where E_A is the activation energy, k is the Boltzmann constant, T is the temperature in Kelvin and σ_0 is the pre-exponential factor. Figure 4.3 shows the activation energy upon salt content. It can be seen that the activation energy for all GPEs are almost the same. From the literature, it is known that the activation energy value for liquid electrolyte is unchanged although the salt concentration changed (Aziz *et al.*, 2015). In this system, GPEs were formed by trapping DMF and EC which is in liquid form at room temperature inside the polymer matrix. Therefore, the activation energy is depending on the nature of the co-solvents (DMF and EC) and thus remains unaffected by the salt concentration.

University of Malaya

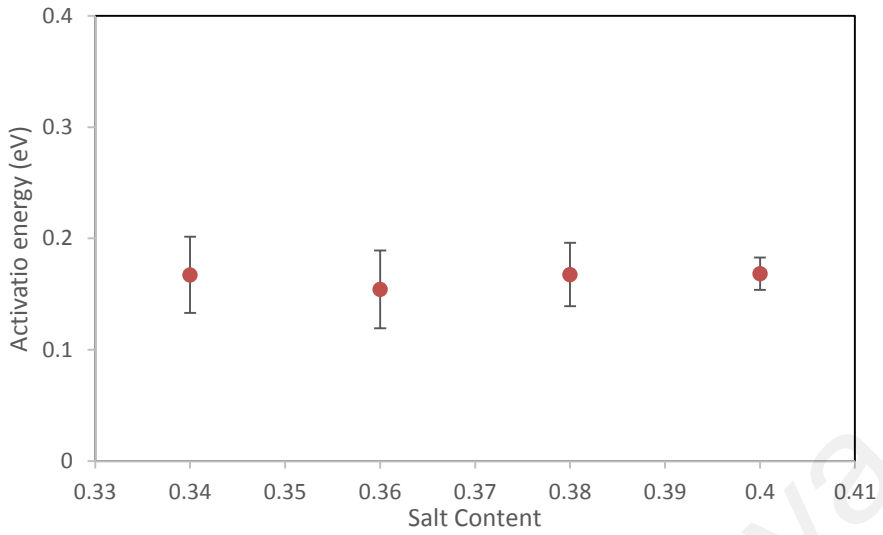

Figure 4.3. Graph of activation energy vs TPAI contents.

4.3 *J-V* Characteristics of DSSCs using PhCh-PEO-DMF-EC-TPAI-I_2 electrolytes

Figure 4.4 shows the *J-V* characteristics for the DSSCs using GPE 1A (SC 1A), GPE 1B (SC 1B), GPE 1C (SC 1C) and GPE 1D (SC 1D) electrolytes. From the figure, it can be seen that the highest J_{sc} was obtained for the DSSC using GPE 1B electrolyte. The higher J_{sc} value may be due to the higher ionic conductivity of the GPE 1B. It is known that the DSSC performance is dependent on few factors such as ionic mobility in the electrolyte. Electrons generated at the photoanode by a sensitizer will be transported to the counter electrode (cathode) and returned back to the photoanode (sensitizer will be regenerated) through the iodide ions (I^-). Once the I^- ion transfers an electron to the sensitizer, it will be transformed to the triiodide (I_3^-) ion which then diffuses to the counter electrode. Therefore, the number density and mobility of I^- and I_3^- ions in the electrolyte are essential for the DSSC performance. The highest J_{sc} obtained was 16.56 mA cm^{-2} for the DSSC using GPE consists of 22.68 wt.% of TPAI (GPE 1B).

The other DSSCs parameters such as V_{oc}, fill factor and efficiency are listed in Table 4.1. As we can see that the DSSC fabricated with 22.68 wt.% of TPAI (GPE 1B) showed the higher conversion efficiency of 7.10 % with J_{sc} = 16.56 mA cm^{-2}, V_{oc} = 0.65 V and

University of Malaya

FF = 0.66. The value of V_{oc} and fill factor are almost same for all DSSC fabricated. Hence, the higher efficiency for SC 1B is due to the higher J_{sc}. In addition, the higher J_{sc} of the cell is attributed to the higher ionic conductivity of iodide and triiodide ions in the GPE. Therefore, the 22.68 wt.% of TPAI (GPE 1B) electrolyte based DSSC (SC 1B) exhibited the highest power conversion efficiency.

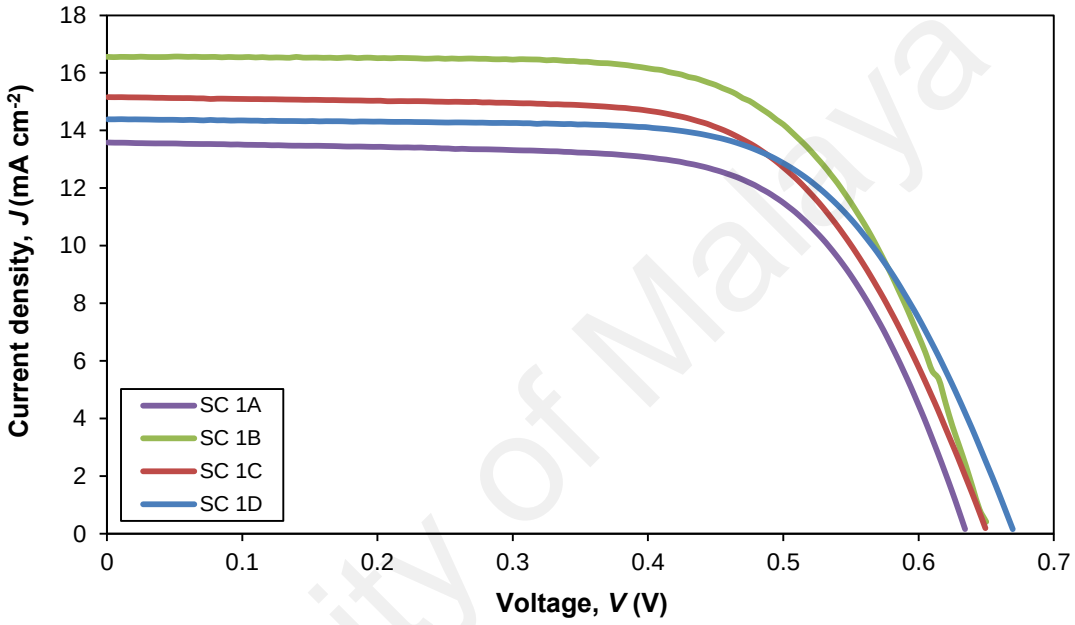

Figure 4.4. *J-V* curves of DSSCs with various amount of TPAI.

Table 4.1. Photovoltaic parameters of DSSCs fabricated with various amount of TPAI.

Electrolyte	DSSCs	J_{sc} (mA cm^{-2})	V_{oc} (V)	Fill Factor, *FF*	Efficiency, η (%)
GPE 1A	SC 1A	13.58	0.63	0.68	5.81
GPE 1B	SC 1B	16.56	0.65	0.66	7.10
GPE 1C	SC 1C	15.15	0.65	0.65	6.40
GPE 1D	SC 1D	14.38	0.67	0.66	6.35

University of Malaya

4.4 Incident photon to current conversion efficiency (IPCE) of DSSCs using PhCh-PEO-DMF-EC-TPAI-I_2 electrolytes

Figure 4.5 shows the graph IPCE measurement with different wavelength of incident light. The IPCE peak of N3 dye-sensitized device is usually at wavelength of 530 nm (Hara *et al.,* 2000) which is comparable with the value obtained in this work (520 to 550 nm). From the figure, it can be observed that the IPCE measurement is following the trend of the GPE conductivity and J_{sc}. It can be seen that the DSSC using 22.68 wt.% of TPAI (GPE 1B) electrolyte exhibits the highest IPCE which is 62 %. The IPCE is defined as the number of electrons in the external circuit collected per incident photon (Wang *et al*., 2014). The relation between J_{sc} and IPCE are shown in equation 4.2:

$$IPCE(\lambda) = 1240 \frac{J_{sc}(\lambda)}{\lambda P_{in}(\lambda)} \qquad (4.2)$$

where P_{in} (λ) (W cm^{-2}) is the incident light and λ (nm) is the wavelength of the incident light. From the equation 4.2, it is clear that the IPCE is proportional to J_{sc}. IPCE increases when the J_{sc} value increases.

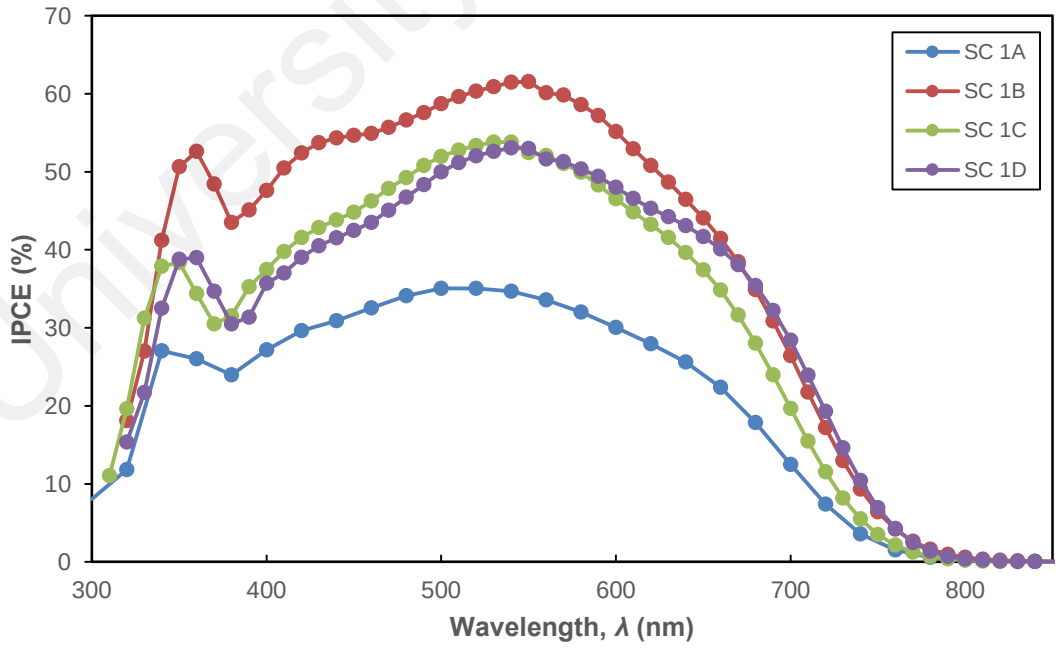

Figure 4.5. IPCE curves of DSSCs with various amount of TPAI salt.

University of Malaya

4.5 Electrochemical impedance spectroscopy (EIS) on DSSCs using PhCh-PEO-DMF-EC-TPAI-I_2 electrolytes

The impedance plots of DSSCs are shown in Figure 4.6. EIS is used to study the movement of electrons at the interfaces in DSSCs.

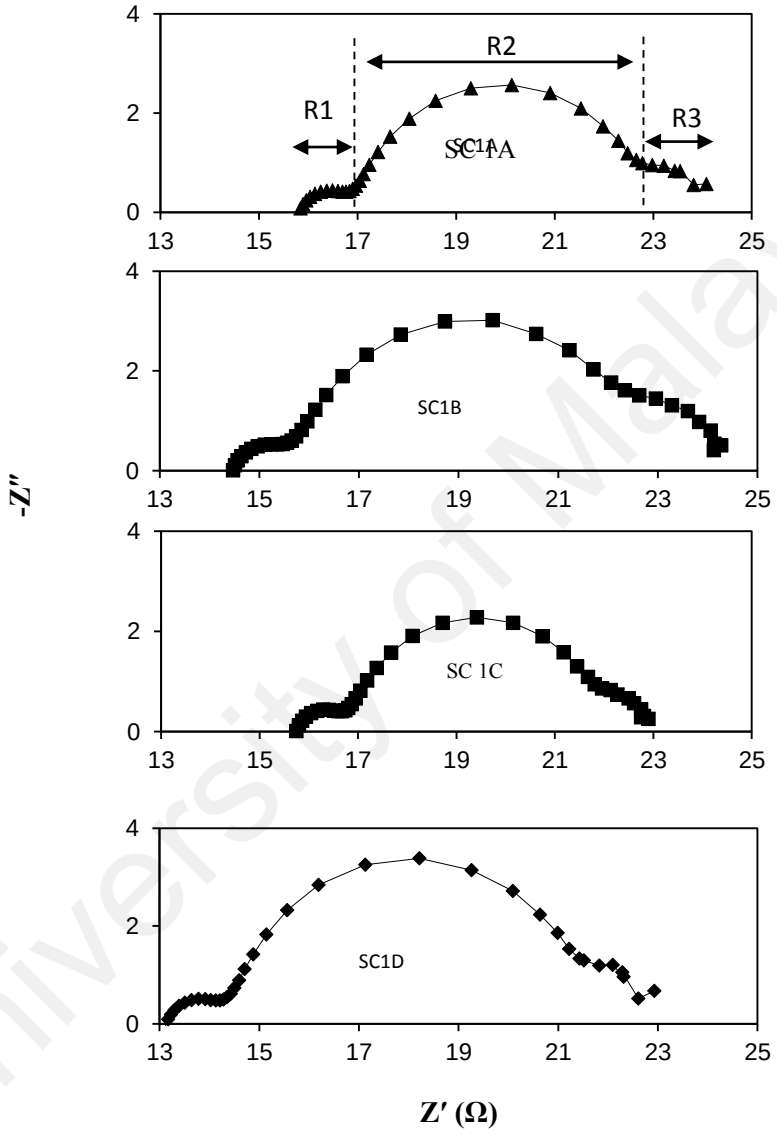

Figure 4.6. Nyquist plots of DSSCs with various amount of TPAI salt.

Usually there are three semicircle observed in impedance plot of DSSC. The first semicircle indicates the charge-transfer resistances at the counter electrode (R1) and the second semicircle corresponds to the charge-transfer resistances of the TiO_2/dye/ electrolyte interface (R2). The third semicircle is associated with the Warburg diffusion

University of Malaya

process of redox couple in the electrolyte (R3). The impedance parameters (R1, R2 and R3) for all DSSCs are listed in Table 4.3. The small R1 value of all DSSCs indicates that the high potential electron transferring from counter electrode to deionized dye (Ma *et al*., 2015). From Table 4.2, it can be observed that the R1 value is almost same for all DSSCs which is due to the same counter electrode used (Pt electrode). The R2 values for all samples follow reversely the trend of power conversion efficiency as shown in Table 4.2. The highest R2 value for SC 1B cell indicates that the electron recombination rate at the dye/TiO_2/electrolyte interface is lower compared to other DSSCs. This leads to higher J_{sc} and efficiency. Meanwhile, DSSCs performance seems not affected by R3 since the value is fluctuating as can be observed from Table 4.2.

Table 4.2. EIS parameters of DSSCs

DSSCs	R1 (Ω)	R2 (Ω)	R3 (Ω)
SC 1A	1.26	5.20	1.80
SC 1B	1.30	6.50	2.05
SC 1C	1.15	4.95	1.15
SC 1D	1.15	4.90	2.69

4.6 Natural dyes as sensitizer

Anthocyanin and chlorophyll dyes were used to fabricate solar cell in order to determine the sequential effect of dipping photoanode into dye materials. Two batches of photo-electrodes were prepared either starting first with anthocyanin or chlorophyll using two sequential dye deposition procedures.

The UV-vis spectrum of the two dyes are shown in Figures 4.7.and 4.8, respectively. The absorption spectrum of anthocyanin dye in methanol solution reveals two peaks at 541 nm and 663 nm.

University of Malaya

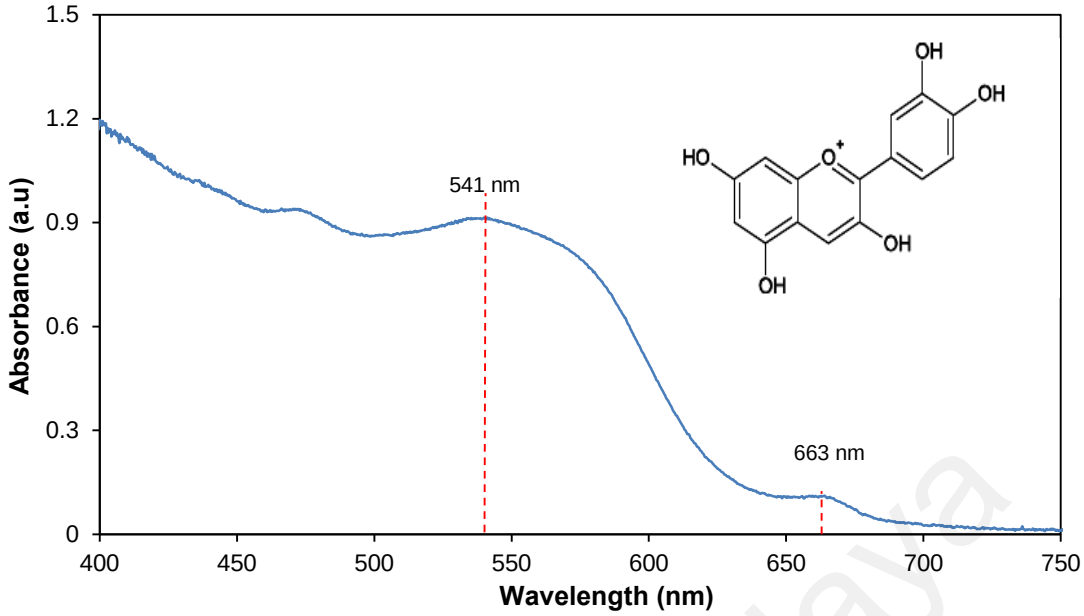

Figure 4.7. UV-vis absorbance curves of anthocyanin dyes.

The chlorophyll dye in methanol solution has shown four absorption peaks at 465 nm, 545 nm, 613 nm and 663 nm, respectively. These absorption wavelength peaks are comparable with reported results (Lim *et al*., 2015).

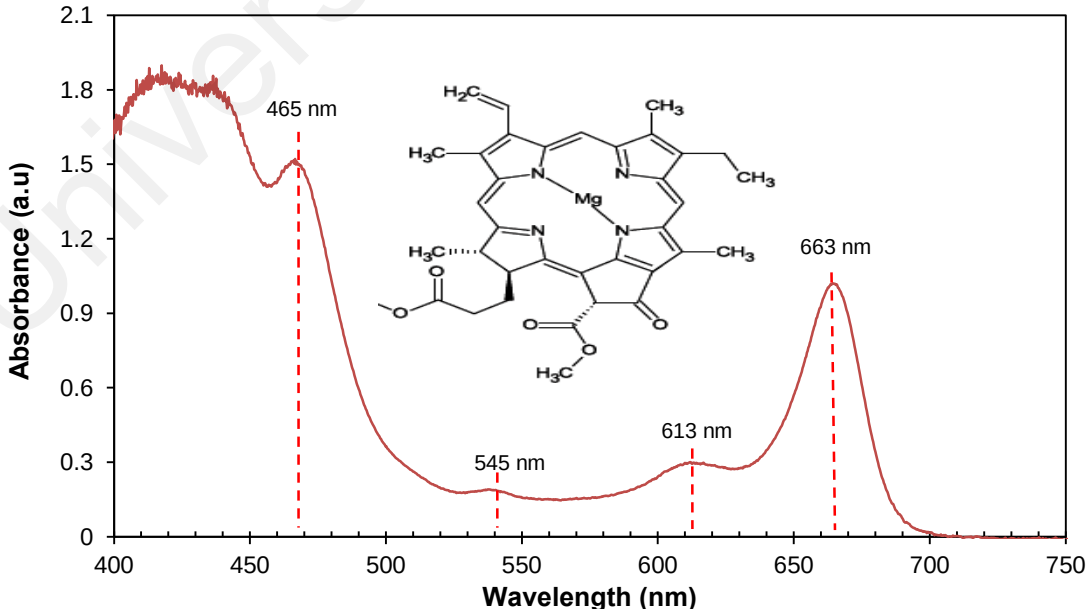

Figure 4.8. UV-vis absorbance curves of chlorophyll dyes.

University of Malaya

GPE with composition of 5.04 wt.% PhCh-1.26 wt.% PEO-37.81 wt.% DMF-31.51 wt.% EC-22.68 wt.% TPAI – 1.70 wt.% I_2 (GPE 1B) is the highest conducting sample and thus used for fabrication of natural DSSCs. The gel electrolyte was sandwiched between the photoanode and counter electrode (Pt).

Figure 4.9 shows the *J–V* curves for the four photoanodes of the DSSCs. The solar cell performances are summarized in Table 4.3. The DSSC using anthocyanin dye (Na1) achieves J_{sc} of 1.83 mA cm^{-2} and efficiency of 0.59 % .On the other hand, DSSC using chlorophyll dye (Na3) achieves J_{sc} of 1.29 mA cm^{-2} and exhibits the efficiency of 0.40 %. These solar cell performances are comparable with the DSSCs performances reported by Melo *et al*. (2009). The DSSC using anthocyanin exhibited higher J_{sc} due to the anthocyanin dye molecules have carbonyl and hydroxyl groups that can easily bind on the surface of TiO_2 and thus electrons can be easily transferred from anthocyanin to the TiO_2 (Theerthagiri *et al*., 2015).

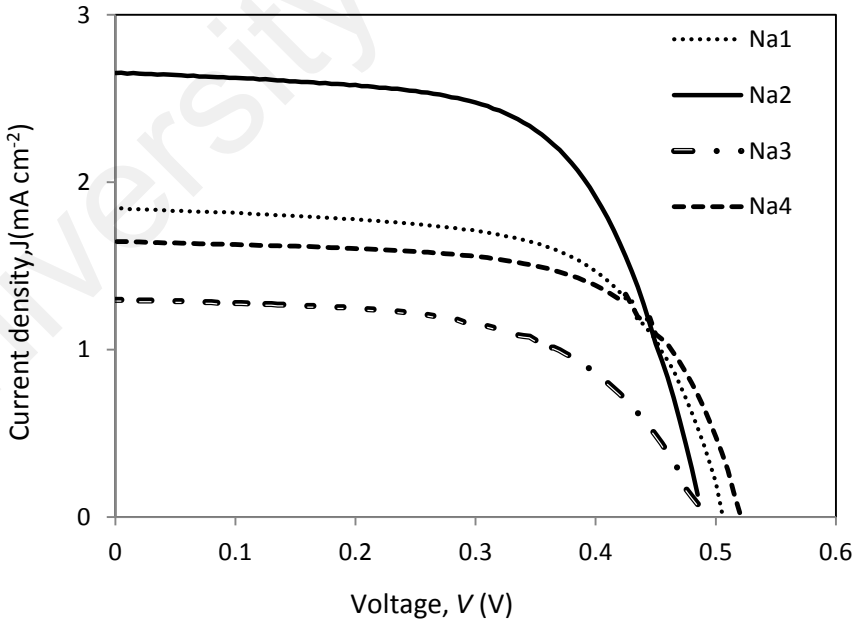

Figure 4.9. *J-V* curves of DSSCs with batch A and batch B photoelectrodes.

University of Malaya

Table 4.3. Performance parameters of DSSCs with batch A and B photoelectrodes.

Dye	DSSCs	J_{sc} (mA cm^{-2})	V_{oc} (V)	Fill Factor, FF	Efficiency, η (%)
Anthocyanin	Na1	1.83	0.50	0.65	0.59
Anthocyanin-Chlorophyll	Na2	2.64	0.49	0.63	0.81
Chlorophyll	Na3	1.29	0.49	0.63	0.40
Chlorophyll-Anthocyanin	Na4	1.64	0.52	0.66	0.56

The Na2 cell (anthocyanin deposited first before chlorophyll) exhibited higher J_{sc} of 2.64 mA cm^{-2} and efficiency of 0.81 % compared to other cells. Also, the J_{sc} and efficiency of Na4 cell is shown to be lower than Na2 cell. Therefore, DSSC performance is enhanced when the anthocyanin dye deposited first before the chlorophyll dye. It is expected that when anthocyanin dye was loaded first, the electrons injection occurs more efficiently into the TiO_2. This is due to the presence of carbonyl and hydroxyl groups in anthocyanin structure that help to produce higher current as well as higher efficiency. Noor *et al*. (2011) have reported an efficiency of 0.42 % for a DSSC with a PVdF-HFP based GPE using mixed dyes (anthocyanin and chlorophyll). In this work, sequential deposition of anthocyanin and chlorophyll dyes showed significant improvement of performance in DSSC application. The IPCE results are illustrated in Figure 4.10.

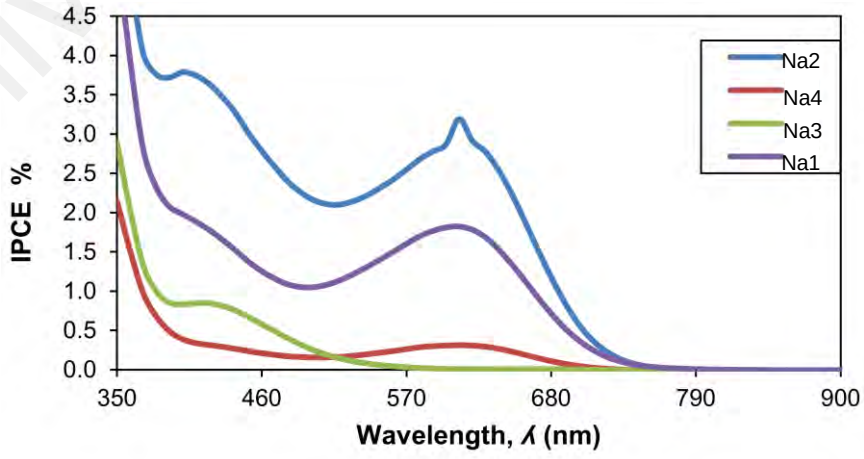

Figure 4.10. IPCE curves of Na1, Na2, Na3 and Na4 cells.

University of Malaya

According to IPCE graph, Na2 cell absorbed more photons that have been converted into electricity as compared to Na1 cell. This is due to Na2 cell contained anthocyanin and chlorophyll dyes, whereas Na1 cell contained only anthocyanin dye. This is attributed to synergistic effect where anthocyanin increased absorption at 500 to 600 nm and chlorophyll dye absorbs at 663 nm. On the other hand, when chlorophyll dye adsorbed first on the semiconductor surface, the chances of anthocyanin dye adsorption is reduced and this leads to the reduced photon conversion efficiency of Na4 cell as compared to Na1 and Na2 cells. Finally, it can be seen that the IPCE value for the Na2 cell is the highest compared to the other cells which is tally with the DSSC results.

Figure 4.11 shows the impedance plots of DSSCs using natural dyes and their parameters (R1 and R2) are listed in Table 4.4. It is observed that the R2 values increase in the order Na2<Na1<Na4<Na3 in four solar cells. The larger semicircle means the higher resistance. The higher resistances for R2 contributed to the lower electron recombination rate.

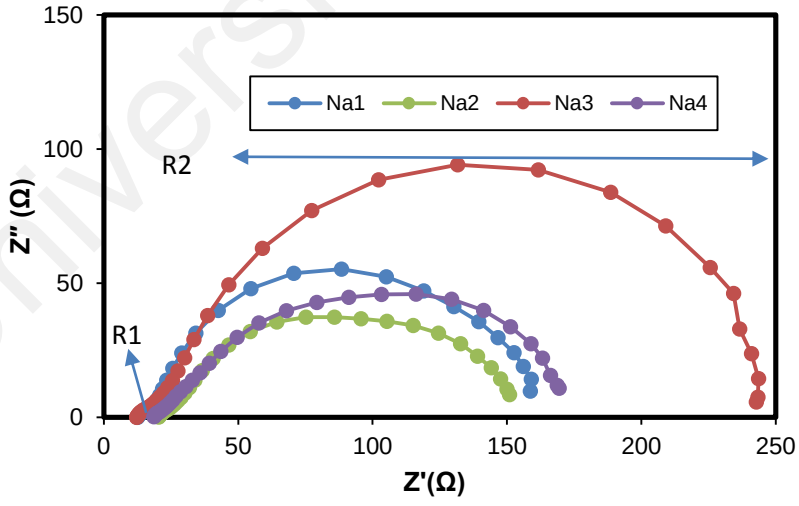

Figure 4.11. The EIS plot of cells Na1, Na2, Na3 and Na4.

University of Malaya

The lower recombination rate is usually good for DSSC. In this DSSC configuration, it can be observed that the highest efficiency cell (Na2) exhibits the highest recombination rate (smallest R2). This may be attributed to the higher electron density in CB of TiO_2 due to higher electron injection from dyes to TiO_2.

Table 4.4. EIS parameters of DSSCs with batch A and B.

DSSCs	R1 (Ω)	R2 (Ω)
Na1	9.15	140.30
Na2	10.68	122.00
Na3	10.07	216.46
Na4	9.56	146.56

4.7 Summary

Various amount of tetrapropylammonium iodide (TPAI) salt was added to optimize the conductivity of gel polymer electrolyte. DSSCs have been assembled with a ruthenium based dye sensitizer. The *J-V* characteristics of the DSSCs have been measured with active area of 0.20 cm^2. The DSSC using an electrolyte containing 22.68 wt. % of TPAI exhibits the highest efficiency of 7.10 % with J_{sc} = 16.56 mA cm^{-2}, V_{oc} = 0.65 V and *FF*= 0.66. The highest conductivity of the electrolyte (22.68 wt. % of TPAI) and also the lowest electrons recombination rate are the reason for the highest efficiency. A series of TiO_2 photoanodes deposited sequentially in anthocyanin and chlorophyll dye sensitizers were tested. The best performance of DSSCs using mixed natural dyes was obtained with the photoelectrode prepared with anthocyanin deposition first then chlorophyll. This cell showed the highest efficiency of 0.81 %. Sequential deposition of dyes on the photoanode can improve the DSSC performance compared to the usage of one or mixture of dyes solution. The better performance is due to the maximum anchoring possibility of anthocyanin dye onto the semiconductor surface together with the increment absorption by chlorophyll.

University of Malaya

CHAPTER 5: Results and Discussions (PhCh-PEO-DMF-EC-TPAI-I_2-TBP)

5.1 Introduction

Phthaloylchitosan (PhCh) blended with polyethylene oxide (PEO) forms the host in gel polymer electrolyte with composition 5.04 wt.% PhCh-1.26 wt.% PEO-31.51 wt.% DMF-37.81 wt.% EC-22.68 wt.% TPAI – 1.70 wt.% I_2 (GPE 1B). To this composition, X wt. % of tert-butyl pyridine (TBP) [X = 2, 4, 6, 8, 10, 12] have been added and the conductivity of the electrolytes has been calculated. DSSCs have been assembled with a ruthenium based dye sensitizer. The *J-V* characteristics, IPCE and impedance of the fabricated DSSCs have been measured.

5.2 The electrical conductivity of PhCh-PEO-DMF-EC-TPAI-I_2-TBP electrolytes

Figure 5.1 shows the Nyquist plot at room temperature for the PhCh-PEO-DMF-EC-TPAI-I_2-TBP GPEs.

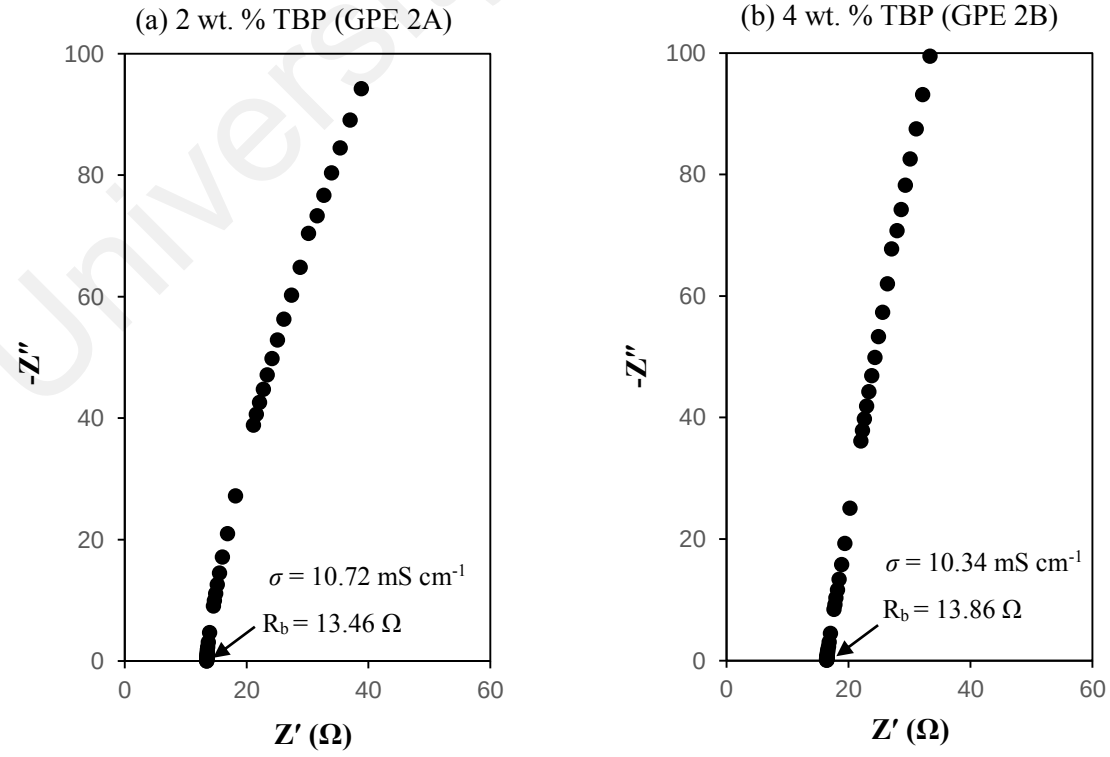

University of Malaya

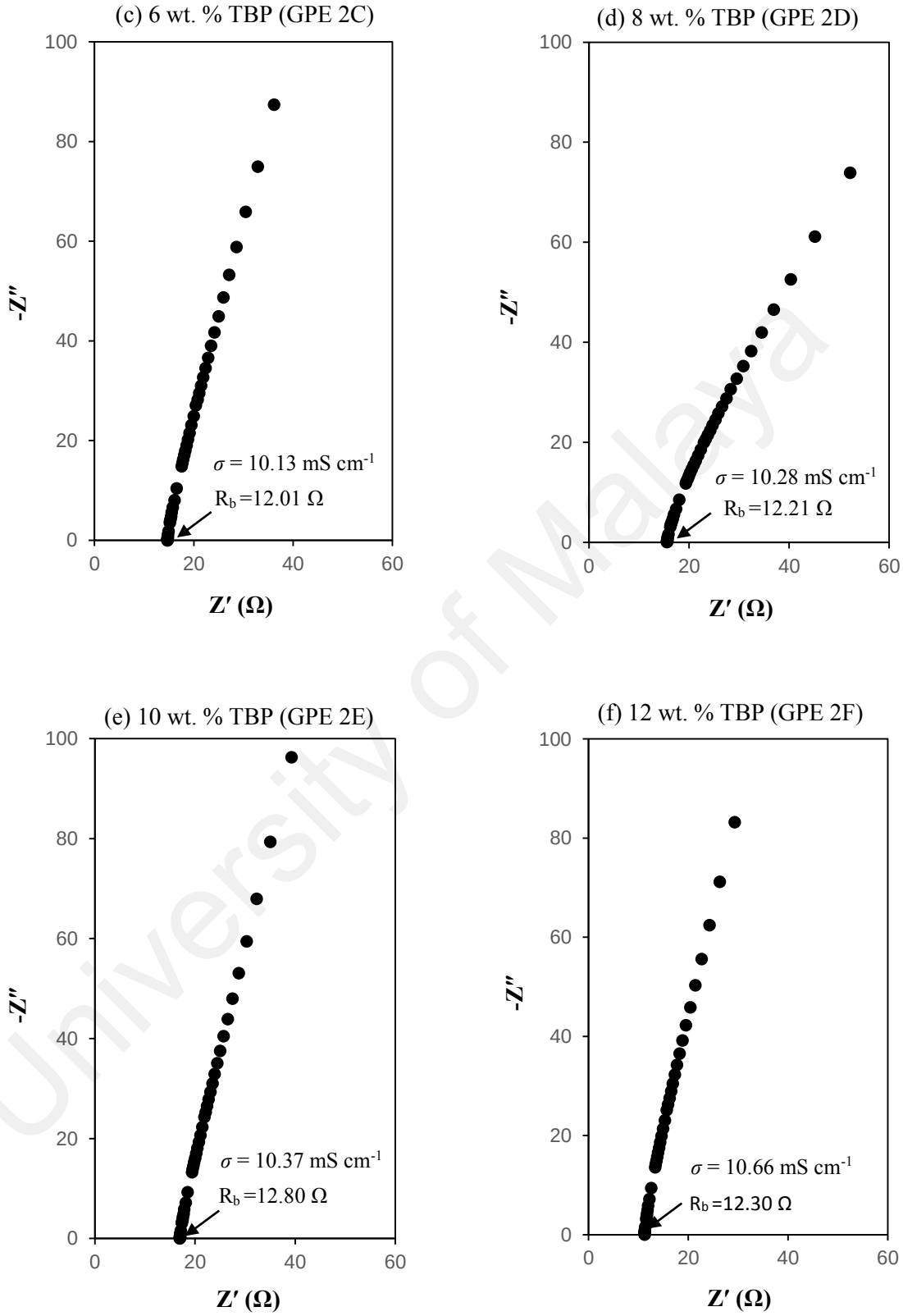

Figure 5.1. Nyquist plot of PhCh-PEO-DMF-EC-TPAI-I_2-TBP GPE.

University of Malaya

From the figure, it can be observed that the spike has been shifted towards right with the addition of TBP indicating the increase in bulk resistance.

The room temperature ionic conductivity of the electrolyte without TBP (GPE 1B) is 11.8 mS cm^{-1}. The ionic conductivity is decreasing in the range from 10.13 to 10.72 mS cm^{-1} as shown in Figure 5.1. The decrease in conductivity is probably due to the less or decrease in salt concentration caused by the addition of TBP. The ionic conductivity of the electrolyte containing 2 wt.% of TBP (GPE 2A) is 10.72 mS cm^{-1}, 4 wt.% TBP (GPE 2B) is 10.34 mS cm^{-1} , 6 wt.% TBP (GPE 2C) is 10.13 mS cm^{-1}, 8 wt.% of TBP (GPE 2D) is 10.28 mS cm^{-1}, 10 wt.% TBP (GPE 2E) is 10.37 mS cm^{-1} and 12 wt.% TBP (GPE 2F) is 10.66 mS cm^{-1}. Figure 5.2 shows the log σ versus 1000/T for PhCh-PEO-DMF-EC-TPAI-I_2-TBP GPE. It can be seen that the conductivity is thermally activated.

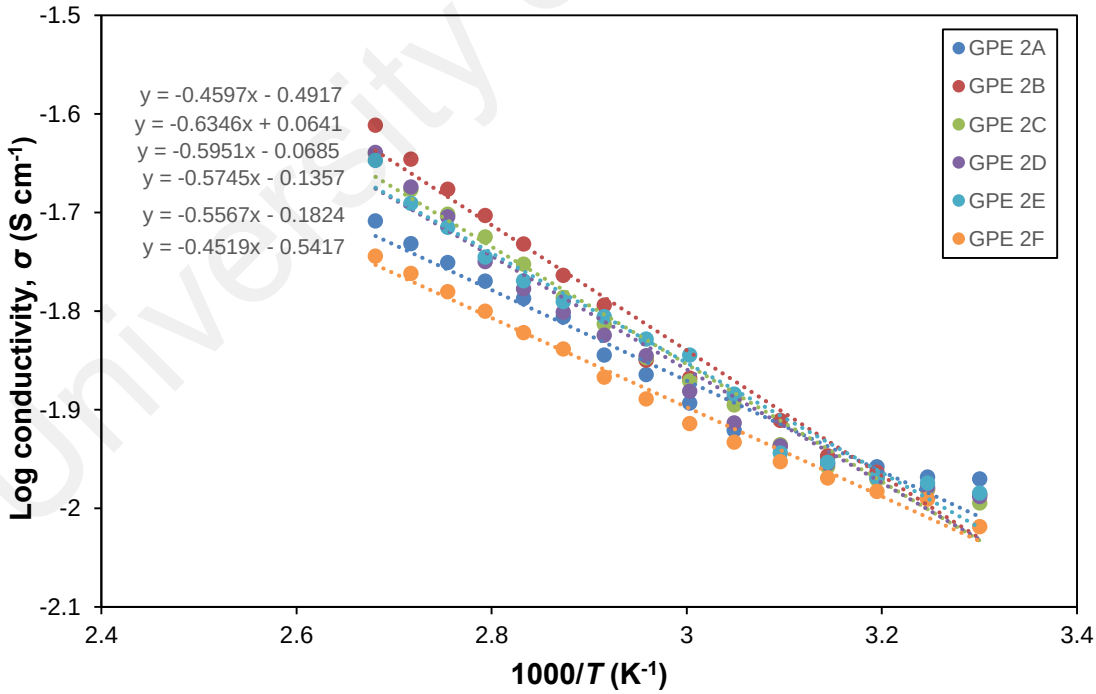

Figure 5.2 Conductivity of gel polymer electrolytes at different temperatures.

University of Malaya

5.3 *J-V* Characteristics of DSSCs using PhCh-PEO-DMF-EC-TPAI-I_2-TBP electrolytes

Figure 5.3 shows the *J–V* curves for DSSCs fabricated using GPE consist of different TBP contents. The sensitizer used is N3 dye. The corresponding performance parameters are listed in Table 5.1. It can be observed that the DSSC with 8 wt. % TBP (GPE 2D) exhibits the highest J_{sc} of 17.30 mA cm^{-2} and an efficiency of 8.84 %. On the other hand, without TBP added in the GPE (GPE 1B), the cell exhibits an efficiency of 7.10 %. The values of V_{oc} and *FF* increase upon addition of TBP which leads to higher efficiency.

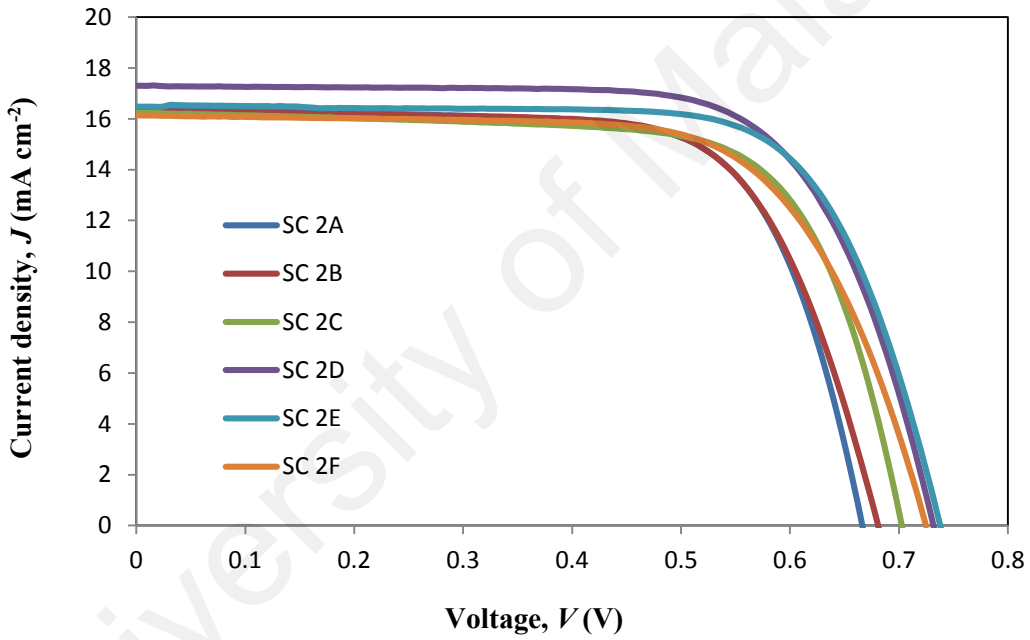

Figure 5.3. *J-V* curves of DSSCs with TBP.

From Table 5.1, it can be observed that the J_{sc} decreased slightly with increasing TBP concentration, but is still not less than 16 mA cm^{-2} except for the cell using 8 wt. % of TBP. The total conversion efficiency increased from 7.68 % for 2 wt. % of TBP to 8.84% for 8 wt. % TBP. Taking into consideration of these results, it is possible that the Fermi level of TiO_2 has shifted to a more negative potential due to the TBP adsorption on the TiO_2 surface that resulted in a large difference between the Fermi level of TiO_2 and redox potential in electrolyte that led to improved V_{oc} (Hara *et al.*, 2003). At a more

University of Malaya

negative potential, charge recombination between electrons injected into TiO_2 and the oxidized N3 dye molecules is possible (Haque *et al.*, 1998). Recombination between injected electrons and triiodide ions is another possible process. All these lead to a reduction in photocurrent. However, it may be implied that the recombination rate is slow since the J_{sc} is still on average greater than 16 mA cm^{-2}. Thus, although the Fermi level has shifted to a more negative potential, but the decreasing leakage of electrons led to almost unchanged value of J_{sc}. As illustrated in Figure 5.3, TBP addition (i) has almost relinquished electron recombination and prevented significant decrease in photocurrent at relatively low voltage and (ii) led to an increase in V_{oc} by increasing the difference in potential between the Fermi and redox levels and (iii) increase *FF* value. It may be considered that the effect of TBP in the electrolyte would be similar to that of semiconducting oxide blocking layers, which prevent the injected electrons from recombining with the triiodide ions. This helps to improve V_{oc} (Zaban *et al*., 2000). The J_{sc} obtained for 8 wt.% of TBP is higher compared to the others. The more dye adsorbed also results in increased light absorption in the photoelectrode and thus giving rise to higher J_{sc}. Moreover, 12 wt.% of TBP may change the band gap of semiconductor materials TiO_2 surface. Therefore, the potential difference between conduction band to valance band will be changed resulting in voltage decreased and fill factor also be reduced.

Table 5.1. Photovoltaic performance parameters of DSSCs with various amount of TBP.

Electrolytes	Cell	J_{sc} (mA cm^{-2})	V_{oc} (V)	Fill Factor, *FF*	Efficiency, η (%)
GPE 2A	SC 2A	16.40	0.66	0.71	7.68
GPE 2B	SC 2B	16.30	0.68	0.70	7.76
GPE 2C	SC 2C	16.23	0.70	0.71	8.06
GPE 2D	SC 2D	17.30	0.73	0.70	8.84
GPE 2E	SC 2E	16.48	0.73	0.73	8.78
GPE2F	SC 2F	16.14	0.72	0.69	8.02

University of Malaya

5.4 Incident photon to current conversion efficiency (IPCE) of DSSCs using PhCh-PEO-DMF-EC-TPAI-I_2-TBP electrolytes

Figure 5.4 shows the IPCE spectrum for DSSCs using PhCh-PEO-DMF-EC-TPAI-I_2-TBP electrolytes. The DSSCs can convert visible light to current efficiently from 300 nm to around 750 nm. The broader IPCE spectrum suggests that the dye molecules have adsorbed effectively to the semiconductor substrate. As can be seen in Figure 5.4, the highest IPCE value is 72.3 % at 530 nm for the cell with 8 wt.% TBP electrolyte. TBP helped to improve IPCE of DSSCs (He *et al*., 2002). He *et al*. (2002) suggested that the co-adsorbents such as TBP reduced surface aggregation that suppressed quenching of dye due to energy transfer between the aggregated molecules. This led to the improved IPCE performance. Khazraji *et al*. (1999) also reported that the IPCE performance of a dye-sensitized TiO_2 solar cell can be improved when added with co-adsorbents. Higher IPCE values indicate effective electron transfer from excited dye molecules to the semiconductors (Hara *et al*., 2000).

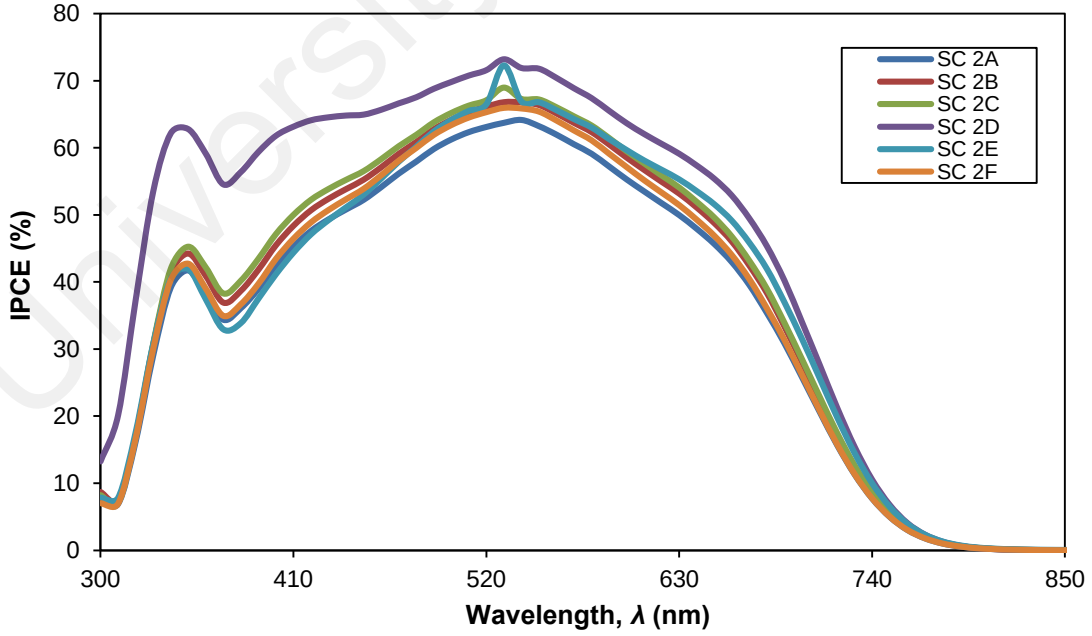

Figure 5.4. IPCE curves of DSSCs with various amount of TBP.

University of Malaya

As can be seen from Figure 5.4, the IPCE measurement of the SC 2A (DSSC using 2 wt.% of TBP electrolyte), SC 2B (DSSC using 4 wt.% of TBP electrolyte), SC 2C (DSSC using 6 wt.% of TBP electrolyte), SC 2E (DSSC using 10 wt.% of TBP electrolyte) and SC 2F (DSSC using 12 wt.% of TBP electrolyte) are quite similar which is around 60 %. However, the IPCE value for SC 2D (DSSC using 8 wt.% of TBP electrolyte) exhibits slightly higher (72 %) compared to the other. This may be due to the charge recombination at the TiO_2/dye/electrolyte interface was suppressed efficiently in the SC 2D cell.

5.5 Electrochemical impedance spectroscopy (EIS) on DSSCs using PhCh-PEO-DMF-EC-TPAI-I_2-TBP electrolytes

The Nyquist plots for the DSSCs with various amount of TBP is shown in Figure 5.5. The R1, R2 and R3 values for the DSSCs using GPE having various amount of TBP is presented in Table 5.2. The increasing R2 value was contributed to reduce electron recombination rate by larger content of adsorbed TBP molecules and more injected electrons could sustain in the conduction band of semiconductor (Jae-yup *et al*., 2012). It means that TBP effect reducing the electron recombination was inclined with the higher contents. This results in higher V_{oc} value as shown Table 5.1. The charge transfer resistance at electrolytes/Pt (R3) also increasing adding TBP indicates deteriorated of platinum interface (Jae-Yup *et al*., 2012).

University of Malaya

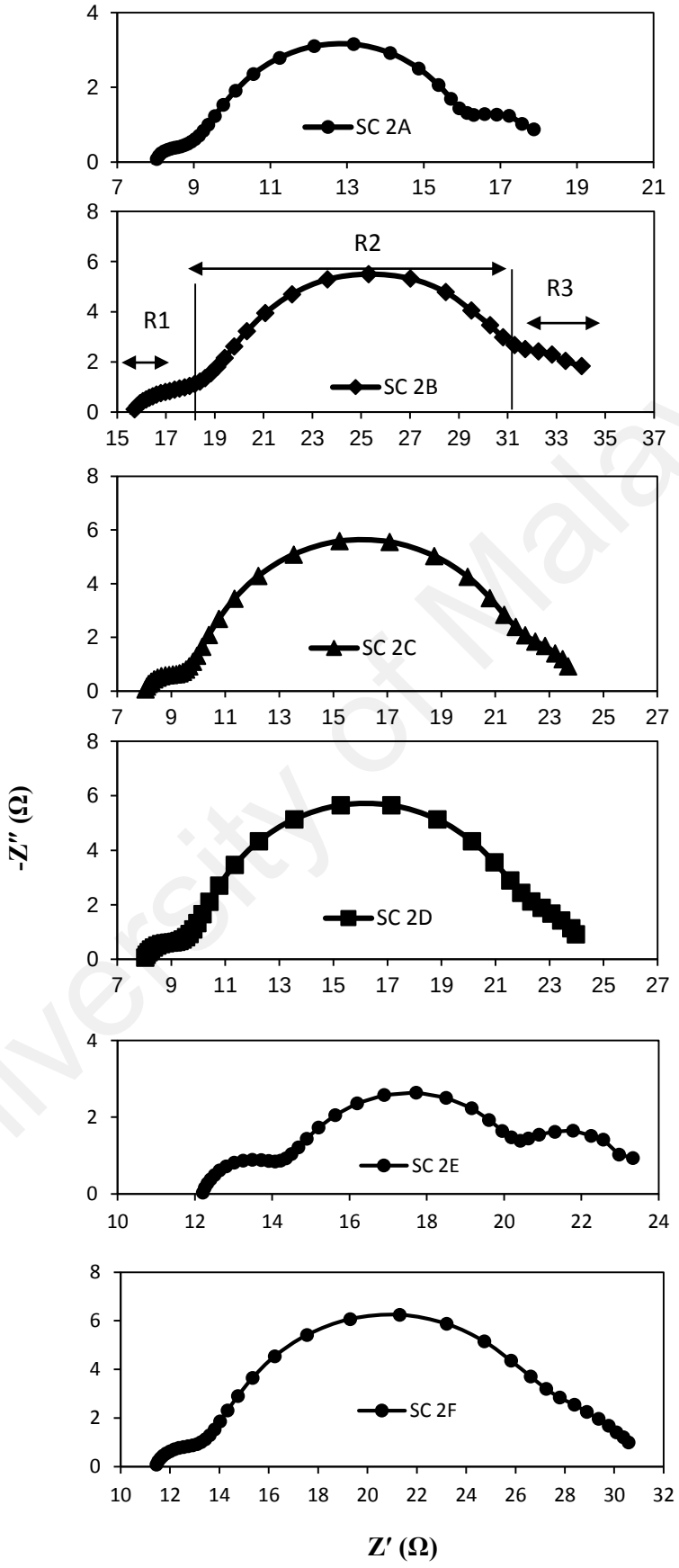

Figure 5.5. Nyquist graphs of solar cells.

University of Malaya

Table 5.2. The R1, R2 and R3 values for the DSSCs with various amount of TBP.

DSSCs	R1 (Ω)	R2 (Ω)	R3 (Ω)
SC 1B	1.30	6.50	2.05
SC 2A	2.22	7.02	2.81
SC 2B	3.16	12.29	3.22
SC 2C	2.93	12.41	3.31
SC 2D	2.63	13.17	3.35
SC 2E	2.25	6.17	2.95
SC 2F	2.64	13.47	3.25

5.6 Summary

The conductivity of gel polymer electrolytes was found to be decreased with the addition of tertbutyl pyridine (TBP). However, the J_{sc} values did not decrease significantly which is due to the suppression of dark current (low electron recombination process). Less electron recombination produces higher $V_{oc.}$ Hence, the overall efficiency of DSSCs having TBP in gel polymer electrolyte has increased. The 8 wt.% TBP containing electrolyte showed the best V_{oc}, FF and efficiency values.

University of Malaya

Chapter 6: Conclusion and suggestions for future work

This dissertation focuses on the optimization of gel polymer electrolyte for the increment of DSSC performance based on natural dyes (anthocyanin and chlorophyll) as well as synthetic dye (N3) as sensitizers. The DSSC structured with one photoanode and a platinized counter electrode (charge collector) coupled with electrolyte in a sandwich form. Optimization work was intensified on TPAI salt based electrolytes and TBP additive based electrolytes. The results of the intensified work was presented and discussed in two chapters (Chapters 4 and 5).

Various amount of tetrapropylammonium iodide (TPAI) salt was added to an optimized phthaloylchitosan (PhCh) based polymer electrolyte. The electrolyte containing 0.36 g of TPAI exhibits the highest efficiency of 7.10 % with J_{sc} = 16.56 mA cm^{-2}, V_{oc} = 0.65 V and FF = 0.66. A series of TiO_2 photoanodes deposited sequentially in anthocyanin and chlorophyll dye sensitizers with various dipping durations have successfully tested. The best performance of DSSCs using mixed natural dyes was obtained with the photoelectrode prepared with anthocyanin deposition first. This cell showed the highest efficiency of 0.81 %. Sequential deposition of dyes on the photoanode can improve the DSSC performance compared to the usage of one or mixture of dyes. The better performance is due to the maximum anchoring possibility of anthocyanin dye onto the semiconductor surface and also increment absorption by chlorophyll.

The addition of TBP in gel polymer electrolytes has further improved the performance of DSSC. Although J_{sc} decreased slightly with increasing TBP content, the total conversion efficiency increased from 7.68 % (2 wt.% of TBP) to 8.84 % (8 wt.% of TBP) before decreased to 8.02 % (12 wt. % of TBP). The improved V_{oc} can be attributed to the suppression of dark current. In further work, the efficiency can be enhanced by incorporating ionic liquid into gel polymer electrolytes in order to improve the ionic conductivity.

University of Malaya

REFERENCES

Alhamed, M., Issa, A., & Doubal, A. (2012). Studying of natural dyes properties as photo-sensitizer for dye sensitized solar cells (DSSC). *Journal of Electron Devices*, *16,* 1370–1383.

Amao, Y., & T. Komori. (2004). Bio-photovoltaic conversion device using chlorine-e6 derived from chlorophyll from Spirulina adsorbed on a nanocrystalline TiO_2 film electrode. *Biosensors Bioelectron*, *19(8),* 843-847.

Aziz, M.F., Buraidah, M.H., Careem, M.A., & Arof. A.K. (2015). PVA based gel polymer electrolytes with mixed iodide salts (K^+ I^- and Bu_4N^+ I^-) for dye-sensitized solar cell application*, Electrochemica acta 182,* 217-223.

Baheti, A., Singh, P., Lee, C.-P., Thomas, K. R. J., & Ho, K.-C. (2011). 2,7-Diaminofluorene-based organic dyes for dye-sensitized solar cells: effect of auxiliary donor on optical and electrochemical properties. *The Journal of Organic Chemistry*, *76(12),* 4910–4920.

Bai, Y., Yu, Q., Cai, N., Wang, Y., Zhang, M., & Wang, P. (2011). ESI: High-efficiency organic dye-sensitized mesoscopic solar cells with a copper redox shuttle. *Chemical Communications (Cambridge, England)*, *47(15),* 4376–4378.

Bella, F., Sacco, A., Salvador, G. P., Bianco, S., Tresso, E., Pirri, C. F., & Bongiovanni, R. (2013). First pseudohalogen polymer electrolyte for dye-sensitized solar cells promising for in situ photopolymerization. *Journal of Physical Chemistry C*, *117(40),* 20421–20430.

Bouchouit, K., Derkowska, B., Migalska-Zalas, A., Abed, S., Benali-cherif, N., & Sahraoui, B. (2010). Nonlinear optical properties of selected natural pigments extracted from spinach: Carotenoids. *Dyes and Pigments*, *86(2),* 161–165.

Boyo, A., Abdulsalami, I. O., Oluwole, S. O., & Umar, A. (2013). Development of Dye Sensitized Solar Cells Using Botuje Green Leaves (Jathopha Curcas Linn). *Science Journal of Physics,* 0–3.

Calogero, G., & Marco, G. Di. (2008). Red Sicilian orange and purple eggplant fruits as natural sensitizers for dye-sensitized solar cells. *Solar Energy Materials and Solar Cells*, *92(11),* 1341–1346.

Chang, H., & Lo, Y. J. (2010). Pomegranate leaves and mulberry fruit as natural sensitizers for dye-sensitized solar cells. *Solar Energy*, *84(10),* 1833–1837.

Chang, H., Kao, M. J., Chen, T. L., Kuo, H. G., Choand, K. C., & Lin, X-P. (2011). Natural sensitizer for dye-sensitized solar cells using three layers of photoelectrode thin films with a Schottky barrier. *American Journal Engineering Applied Science 4(2),* 214–222.

Chiba, Y., Islam, A., Watanabe,Y., Komiya, R., Koide, N., & Han, L.(2006). Natural Chlorophyll-Related Porphyrins and Chlorins for Dye-Sensitized Solar Cells. *Japan Journal Applied Physics, 45,* 638-640.

Chiron, J., Clifford, J. N., Joly, D., Pelleja, L., Palomares, E., & Demadrille, R. (2014). A Robust Organic Dye for Dye Sensitized Solar Cells Based on Iodine / Iodide Electrolytes Combining High Efficiency. *Scientific reports, 4(1-7),* 4033.

University of Malaya

Chen, C. Y., Wang, M., Li, J. Y., Pootrakulchote, N., Alibabaei, L., Ngoc-Le, C. H., Grätzel, M. (2009). Highly efficient light-harvesting ruthenium sensitizer for thin-film dye-sensitized solar cells. *American chemical society Nano*, *3(10),* 3103–3109.

Chen, C. L., Chang, T. W., Su, S. C., Teng, H., & Lee, Y. L. (2014). High performance solid-state dye-sensitized solar cells based on poly(acrylonitrile-co-vinyl acetate)/TiO_2 nanoparticles redox electrolytes. *Power Sources*, *247,* 406–411.

Cho, T. Y., Ko, K. W., Yoon, S. G., Sekhon, S. S., Kang, M. G., Hong, Y. S., & Han, C. H. (2013). Efficiency enhancement of flexible dye-sensitized solar cell with sol-gel formed Nb_2O_5 blocking layer. *Current Applied Physics*, *13(7),* 1391–1396.

Choi, H., Kim, S., Kang, S. O., Ko, J., Kang, M.-S., Clifford, J. N., Forneli, A., Palomares, E., Nazeeruddin, M. K., & Gra¨tzel, M.(2008). Stepwise cosensitization of nanocrystalline TiO_2 films utilizing Al2O3 layers in dye-sensitized solar cells. *Angew. Chemistry, 120,* 8383 –8387.

Chou, C.-S., Chou, F.-C., & Kang, J.-Y. (2012). Preparation of ZnO-coated TiO_2 electrodes using dip coating and their applications in dye-sensitized solar cells. *Powder Technology*, (*215–216),* 38–45.

Clifford, J. N., Palomares, E., Nazeeruddin, M. K., Thampi, R., Grätzel, M., & Durrant, J. R. (2004). Multistep Electron Transfer Processes on Dye Co-sensitized Nanocrystalline TiO_2 Films. *American Chemical Society*, *126(18),* 5670–5671.

Cui, Y., Zhang, X., Feng, J., Zhang, J., & Zhu, Y. (2013). Enhanced photovoltaic performance of quasi-solid-state dye-sensitized solar cells by incorporating a quaternized ammonium salt into poly(ethylene oxide)/poly(vinylidene fluoride-hexafluoropropylene) composite polymer electrolyte. Electrochimica Acta, *108,* 757–762.

Daeneke, T., Kwon, T. H., Holmes, A. B., Duffy, N. W., Bach, U., & Spiccia, L. (2011). High-efficiency dye-sensitized solar cells with ferrocene-based electrolytes. *Nature Chem*istry, *3 (3),* 211–215.

Deacon, G. B., & Phillips, R. J. (1980). Relationship between the carbon-oxygen stretching frequencies of the carboxylate complexes and the type of carboxylate coordination. *Coordination Chemistry Re*views*, 33(3),* 227-250.

Dentani, T., Kubota, Y., Funabiki, K., Jin, J., Yoshida, T., Minoura, H., Miura,H., Matsui, M. (2009). Novel thiophene-conjugated indoline dyes for zinc oxide solar cells. *New Journal of Chemistry*, *33(1),* 93–101.

Dissanayake, M. A. K. L., Thotawatthage, C. A., Senadeera, G. K. R., Bandara, T. M. W. J., Jayasundera, W. J. M. J. S. R., & Mellander, B. E. (2012). Efficiency enhancement by mixed cation effect in dye-sensitized solar cells with PAN based gel polymer electrolyte. *Journal of Photochemistry and Photobiology A: Chemistry*, *246,* 29–35.

University of Malaya

Ehret, A., Stuhl, L., & Spitter, M.T. (2001). Spectral sensitization of TiO_2 nanocrystalline electrodes with aggregated cyanine dyes. *Journal physical Chemistry B, 105*, 9960-9965.

Erten-Ela, S., Yilmaz, M. D., Icli, B., Dede, Y., Icli, S., & Akkaya, E. U. (2008). A panchromatic boradiazaindacene (BODIPY) sensitizer for dye-sensitized solar cells. *Organic Letters*, *10(15),* 3299–3302.

Fabregat-Santiago, F., Barea, E. M., Bisquert, J., Mor, G. K., Shankar, K., & Grimes, C. A. (2008). High carrier density and capacitance in TiO2 nanotube arrays induced by electrochemical doping. *Journal of the American Chemical Society*, *130(34),* 11312–11316.

Fang, X., Ma, T., Guan, G., Akiyama, M., Kida, T., & Abe, E. (2004). Effect of the thickness of the Pt film coated on a counter electrode on the performance of a dye-sensitized solar cell. *Journal of Electroanalytical Chemistry*, *570(2),* 257–263.

Ferrere, S., Zaban, A., & Gregg, B. a. (1997). Dye Sensitization of Nanocrystalline Tin Oxide by Perylene Derivatives. *Journal Physical Chemistry B*, *5647(97),* 4490–4493.

Frank,T (2005). Pharmacokinetics of anthocyanidin-3-glycosides following consumption of Hibiscus sabdariffa L. extract. *Journal Clinical Pharmacol*ogy, *45(3),* 203–210.

Fukai, Y., Kondo, Y., Mori, S., & Suzuki, E. (2007). Highly efficient dye-sensitized SnO_2 solar cells having sufficient electron diffusion length. *Electrochemistry Communications*, *9(7),* 1439–1443.

Furukawa, S., Iino, H., Iwamoto, T., Kukita, K., & Yamauchi, S. (2009). Characteristics of dye-sensitized solar cells using natural dye. *Thin Solid Films*, *518(2),* 526–529.

Ganesan, S., Muthuraaman, B., Mathew, V., Vadivel, M. K., Maruthamuthu, P., Ashokkumar, M., & Suthanthiraraj, S. A. (2011). Influence of 2,6 (N-pyrazolyl)isonicotinic acid on the photovoltaic properties of a dye-sensitized solar cell fabricated using poly(vinylidene fluoride) blended with poly(ethylene oxide) polymer electrolyte. *Electrochimica Acta*, *56(24),* 8811–8817.

Ganesan, S., Muthuraaman, B., Madhavan, J., Mathew, V., Maruthamuthu, P., & Suthanthiraraj, S. A. (2008). The use of 2,6-bis (N-pyrazolyl) pyridine as an efficient dopant in conjugation with poly(ethylene oxide) for nanocrystalline dye-sensitized solar cells. *Electrochimica Acta*, *53(27),* 7903–7907.

Gao, F., Wang, Y., Shi, D., Zhang, J., Wang, M., Jing, X., Humphry-Baker, R., Wang, P., Zakeeruddin, S. M., & Grätzel, M. (2008). Enhance the Optical Absorptivity of Nanocrystalline TiO_2 Film with High Molar Extinction Coefficient Ruthenium Sensitizers for High Performance Dye-Sensitized Solar Cells. *Journal American Chemical Society, 130(32),* 10720-10728.

Garcia, C. G., Sarto Polo, A., & Murakami Iha, N. Y. (2003). Fruit extracts and ruthenium polypyridinic dyes for sensitization of TiO_2 in photoelectrochemical solar cells. *Journal of Photochemistry and Photobiology A: Chemistry*, *160(1–2),* 87–91.

University of Malaya

Gómez-Ortíz, N. M., Vázquez-Maldonado, I. A., Pérez-Espadas, A. R., Mena-Rejón, G. J., Azamar-Barrios, J. A., & Oskam, G. (2010). Dye-sensitized solar cells with natural dyes extracted from achiote seeds. *Solar Energy Materials and Solar Cells*, *94(1),* 40–44.

Gong, F., Wang, H., Xu, X., Zhou, G., & Wang, Z. S. (2012). In situ growth of $Co_{0.85}Se$ and $Ni_{0.85}Se$ on conductive substrates as high-performance counter electrodes for dye-sensitized solar cells. *American Chemical Society, 134(26),* 10953–10958.

Grätzel. M. (1995). Low Cost and Efficient Photovoltaic Conversion by Nanocrystalline Solar Cells. *Chemie Ingenieur Technik*, *67(10),* 1300–1305.

Green, M.A. (1982). Solar cells: operating principles, technology, and system applications. United States: *Prentice-Hall, Inc.,Englewood Cliffs*, NJ.

Grotewold , E. (2006). The science of flavonoids: Columbus, Springer. USA, 273.

Hagfeldt, A., Boschloo, G., Sun, L., Kloo, L., & Pettersson, H. (2010). Dye-sensitized solar cells. *Chemical Reviews, 110(11),* 6595–6663.

Han, D.W., Heo, J. H., Kwak, D. J., Han, C. H., & Sung,Y. M. (2009). Texture, morphology and photovoltaic characteristics of nanoporous F: SnO_2 films. *Journal of Electrical Engineering and Technology*, *4(1),* 93–97.

Hao, S., Wu, J., Huang, Y., & Lin, J. (2006). Natural dyes as photosensitizers for dye-sensitized solar cell. *Solar Energy*, *80(2),* 209–216.

Haque, S. A., Yachibana, Y.,Klug, D. R., & Durrant, J. R. (1998). Charge Recombination Kinetics in Dye-Sensitized Nanocrystalline Titanium Dioxide Films under Externally Applied Bias. *Physical Chemistry B, 102(10),* 1745-1749.

Hara, K., Dan-oh, Y., Kasada, C., Ohga, Y., Shinpo, A., Suga, S., Arakawa, H. (2004). Effect of additives on the photovoltaic performance of coumarin-dye-sensitized nanocrystalline TiO_2 solar cells. *Langmuir : The ACS Journal of Surfaces and Colloids*, *20(10),* 4205–4210.

Hara, K., Horiguchi, T., Kinoshita, T., Sayama, K., Sugihara, H., & Arakawa, H. (2000). Highly efficient photon-to-electron conversion with mercurochrome-sensitized nanoporous oxide semiconductor solar cells. *Solar Energy Materials and Solar Cells, 64(2),* 115–134.

Hara, K., Kurashige, M., Dan-oh, Y., Kasada, C., Shinpo, A., Suga, S., Sayama, K., & Arakawa, H. (2003). Design of new coumarin dyes having thiophene moieties for highly efficient organic-dye-sensitized solar cells. *New Journal Chemistry, 27(5),* 783-785.

Hara, K., Sayama, K., Ohga, Y., Shinpo, A., Suga, S., & Arakawa, H. (2001). A coumarin-derivative dye sensitized nanocrystalline TiO_2 solar cell having a high solar-energy conversion efficiency up to 5.6%. *Chemistry Communication, 10(6),* 569-570.

Hardin, B. E., Snaith, H. J., & McGehee, M. D. (2012). The renaissance of dye sensitized solar cells, *nature photonics*, *6(3),* 6162–169.

University of Malaya

Hassan, H. C., Abidin, Z. H. Z., Careem, M. A. &. Arof. A. K. (2014). Chlorophyll as sensitizer in I^-/I_3^- based solar cells with quasi-solid-state electrolytes. *High Performance Polymers. 26(6),* 647–652.

He, J., Benkö, G., Korodi, F., Polívka, T., Lomoth, R., Åkermark, B., Sundström, V. (2002). Modified phthalocyanines for efficient near-IR sensitization of nanostructured TiO2 electrode. *American Chemical Society, 124(17),* 4922–4932.

Hemalatha, K. V., Karthick, S. N., Justin Raj, C., Hong, N. Y., Kim, S. K., & Kim, H. J. (2012). Performance of Kerria japonica and Rosa chinensis flower dyes as sensitizers for dye-sensitized solar cells. *Spectrochimica Acta - Part A: Molecular and Biomolecular Spectroscopy*, *96,* 305–309.

Higashino, T., & Imahori, H. (2015). Porphyrins as excellent dyes for dye-sensitized solar cells: recent developments and insights. *Dalton Transactions, 44(2),* 448–463.

Isah Kimpa, M. (2012). Photoelectric Characterization of Dye Sensitized Solar Cells Using Natural Dye from Pawpaw Leaf and Flame Tree Flower as Sensitizers. *Materials Sciences and Applications*, *3,* 281–286.

Kakiage, K., Aoyama, Y., Yano, T., Oya, K., Fujisawa, J.I., & Hanaya, M. (2015). Highly-Efficient Dye-Sensitized Solar Cells with Collaborative Sensitization by Silyl-Anchor and Carboxy-Anchor Dyes. *Chemistry Communication, 51(88),* 15894–15897.

Kalyanasundaram, K., & Gra¨tzel, M. (1998). Applications of functionalized transition metal complexes in photonic and optoelectronic devices. *Coordinate Chemical Re*views*, 117(1),* 347-414.

Kamel, M. M., El-Shishtawy, R. M, Yussef, B. M., & Mashaly, H. (2005). Ultrasonic assisted dyeing: III. Dyeing of wool with lac as a natural dye. *Dyes and Pigment*, *65(2),* 103–110.

Kartini,I., Dwitasari.L., Wahyuningsih ,T. D., Chotimah.C., & Wang, L. (2015). The Sensitization of Xanthophylls-Chlorophyllin Mixtureson Titania Solar Cells. *International Journal Science Eng*ineering, *8(2),* 109-114.

Kato, F., Kikuchi, A., Okuyama, T., Oyaizu, K., & Nishide, H. (2012). Nitroxide radicals as highly reactive redox mediators in dye-sensitized solar cells. *Angewandte Chemie - International Edition*, *51(40),* 10177–10180.

Keka, S., Saha, P.D., & Datta, S. (2012). Extraction of natural dye from etals Flam of forest (Butea monosperma) flower: process optimization using response surface methodology (RSM). *Dyes and Pigment*, *94(2),* 212–216.

Khazraji, A. C., Hotchandani, S., Das, S., & Kamat, P. V. (1999). Controlling Dye (Merocyanine-540) Aggregation on Nanostructured TiO_2 Films. An Organized Assembly Approach for Enhancing the Efficiency of Photosensitization. *Physical Chemistry B*, *103,* 4693–4700.

University of Malaya

Kim, J. Y., Kim, J. Y., Lee, D. K., Kim, B., Kim, H., & Ko, M. J. (2012). Importance of 4- tert-butylpyridine in electrolyte for dye-sensitized solar cells employing SnO 2 electrode. *Physical Chemistry C*, *116(43),* 22759–22766.

Kishiomoto, S., Maoka, T., Sumitomo, K., & Ohmya, A. (2005). Analysis of carotenoid composition in petals of calendula (Calendula officinalis L). *Biosci Biotechnol Biochem*, *69(11)*2122–2128.

Konczak, I., & Zhang, W. (2004). Anthocyanins—More Than Nature's Colours. *Biomedicine and Biotechnology*, *5,* 239–240.

Kouissa, B., Bouchouit, K., Abed, S., Essaidi, Z., Derkowska, B., & Sahraoui, B. (2013). Investigation study on the nonlinear optical properties of natural dyes: Chlorophyll a and b. *Optics Communications*, *293,* 75–79.

Koyama, Y., Kakitani, Y., & Nagae, H. (2012). Mechanisms of suppression and enhancement of photocurrent/conversion efficiency in dye-sensitized solar-cells using carotenoid and chlorophyll derivatives as sensitizers. *Molecules*, *17(2),* 2188–2218.

Kumara, G. R. A., Kaneko, S., Okuya, M., Onwona-Agyeman, B., Konno, A., & Tennakone, K. (2006). Shiso leaf pigments for dye-sensitized solid-state solar cell. *Solar Energy Materials and Solar Cells*, *90(9),* 1220–1226.

Kumara, G. R. R. a, Tennakone, K., Perera, V. P. S., Konno, a, Kaneko, S., & Okuya, M. (2001). Suppression of recombinations in a dye-sensitized photoelectrochemical cell made from a film of tin IV oxide crystallites coated with a thin layer of aluminium oxide. *Journal of Physics D: Applied Physics*, *34,* 868–873.

Kung, C.-W., Chen, H.-W., Lin, C.-Y., Huang, K.-C., Vittal, R., & Ho, K.-C. (2012). CoS Acicular Nanorod Arrays for the Counter Electrode of an efficient dye-sensitized solar cell. *American chemical society,Nano*, *6(8),* 7016–7025.

Kuppuswamy, K., & Grätzel**,** M. (2009). Efficient Dye-Sensitized Solar Cells for Direct Conversion of Sunlight to Electricity, *Material Matters. 4(4),* 88.

Kusama, H., Orita, H., & Sugihara, H. (2008). TiO_2 Band Shift by Nitrogen-Containing Heterocycles in Dye-Sensitized Solar Cells: a Periodic Density Functional Theory Study. *Langmuir*, *24(8),* 4411– 4419.

Lee, K. M., Suryanarayanan, V., & Ho, K. C. (2009). Influences of different TiO_2 morphologies and solvents on the photovoltaic performance of dye-sensitized solar cells.*Power Sources*, *188(2),* 635–641.

Li, C., Yang, X., Chen, R., Pan, J., Tian, H., Zhu, H., Wang, X., Hagfeldt, A., & Sun, L. (2007). Anthraquinone dyes as photosensitizers for dye-sensitized solar cells. Solar Energy Materials and Solar Cells. *Sol. Energy Mater. Sol. Cells*, *91(19),* 1863-1871.

Li, G. R., Wang, F., Jiang, Q. W., Gao X. P. & Shen, P. W. (2010). Carbon nanotubes with titanium nitride as a low cost counter electrode material for dye sensitized solar cells. *Angew. Chemical International (Ed.*), *49(21),* 3653–3656.

University of Malaya

Li, Y., Ku, S. H., Chen, S. M., Ali, M. A., & AlHemaid, F. M. A. (2013). Photoelectrochemistry for red cabbage extract as natural dye to develop a dye-sensitized solar cells. *Electrochemical Science*, *8*(1), 1237–1245.

Li, Y., Li, X., Guo, H., Wang,Z., & Li, T.(2014). Effect on properties of PVDF-HFP based composite polymer electrolyte doped with nano-SiO_2 .*Iran Polymer, 23(6),* 487-494.

Lim ,A., Manaf, N. H., Tennakoon, K., Chandrakanthi, R. L. N., Lim ,L. B. L., Bandara, J. M. R. S., & Ekanayake ,P. (2015). Higher Performance of DSSC with Dyes from Cladophora sp. as Mixed Cosensitizer through Synergistic Effect. *Biophysics*, *1-8,* 510467.

Liu, X., Zhu, R., Zhang, Y., Liu, B., & Ramakrishna, S. (2008). Anionic benzothiadiazole containing polyfluorene and oligofluorene as organic sensitizers for dye-sensitized solar cells. *Chemical Communications (Cambridge, England)*, *(32),* 3789–91.

Liu, Y., Jennings, J. R. & Wang, Q. (2013). Efficient dye-sensitized solar cells using a tetramethylthiourea redox mediator, *Sustainable Chemistry*, *6(11),* 2124–2131

Liu, Y., Hagfeldt, A., Xiao, X.-R., & Lindquist, S.-E. (1998). Investigation of influence of redox species on the interfacial energetics of a dye-sensitized nanoporous TiO_2 solar cell. *Solar Energy Materials and Solar Cells*, *55*(February), 267–281.

Lu, M., Liang, M., Han, H. Y., Sun, Z., & Xue, S. (2011). Organic dyes incorporating bis-hexapropyltruxeneamino moiety for efficient dye-sensitized solar cells. *Physical Chemistry C*, *115(1),* 274–281.

Luo, P., Niu, H., Zheng, G., Bai, X., Zhang, M., & Wang, W. (2009). From salmon pink to blue natural sensitizers for solar cells: Canna indica L., Salvia splendens, cowberry and Solanum nigrum L. *Spectrochimica Acta - Part A: Molecular and Biomolecular Spectroscopy*, *74(4),* 936–942.

Ma, X., Yue, G., Wu, J., & Lan,Z.(2015). Efficient Dye-Sensitized Solar Cells Made from High Catalytic Ability of Polypyrrole@Platinum Counter Electrode. *Nanoscale Research Letters*, *10(1),* 1115.

Mathew, S., Yella, A., Gao, P., Humphry-Baker, R., Curchod, B. F. E., Ashari-Astani, N., Tavernelli, I. U., Rothlisberger, Nazeeruddin, M. K., & Grätzel, M. (2014). Dye-sensitized solar cells with 13% efficiency achieved through the molecular engineering of porphyrin sensitizers. *Nature Chemistry*, *6(3),* 242–247.

Mehmood, U., Rahman, S., Harrabi, K., Hussein, I. A., & Reddy, B. V. S. (2014). Recent Advances in Dye Sensitized Solar Cells. *Advances in Materials Science and Engineering*, *2014,* 1–12.

Melo, M.J., Pina , F. , Andary, C., Bechtold, T., & Mussak(Eds.) , R. (2009). Handbook of Natural colourants, *John Wiley & Sons, Ltd*., United Kingdom, 135-150.

University of Malaya

Mishra, A., Fischer, M. K. R., & Bauerle, P. (2009). Metal-free organic dyes for dye-sensitized solar cells: from structure: property relationships to design rules. *Angew. Chemical International (Ed.) 48(14),* 2474-2499.

Mohamed, N. S., & Arof, A. K. (2004). Investigation of electrical and electrochemical properties of PVDF-based polymer electrolytes. *Power Sources*, *132(1–2),* 229–234.

Mohan, V. M., & Murakami, K. (2011). Dye sensitized solar cell with carbon doped (PAN/PEG) polymer quasi-solid gel electrolyte. *Advanced Research in Physics*, *2(2),* 1–6.

Muthuraaman, B., Will, G., Wang, H., Moonie, P., & Bell, J. (2013). Increased charge transfer of Poly (ethylene oxide) based electrolyte by addition of small molecule and its application in dye-sensitized solar cells. *Electrochimica Acta*, *87,* 526–531.

Narayan, M., & Raturi, A. (2011). Investigation of some common Fijian flower dyes as photosensitizers for dye Sensitized Solar Cellsabstract. *Applied Solar Energy*, *47(2),* 112–117.

Nguyen, T. V., Lee, H. C., Alam Khan, M., & Yang, O. B. (2007). Electrodeposition of TiO_2/SiO_2 nanocomposite for dye-sensitized solar cell. *Solar Energy*, *81(4),* 529–534.

Nazzerruddin, M. K., Kay,A., Podicio,I., Humphy-Baker,R., Müller,E., Liska,P., Nguyen, T.V., Lee, H.C., Khan, M. A., & Yang,O.B. (2007). Electrodeposition of TiO_2/SiO_2 nanocomposite for dye-sensitized solar cell. *Solar Energy*. *81(4),* 529–534.

Nazeeruddin, M. K., Kay.A. , Rodicio,L., Humphry-Baker,R., Mueller,E., Liska,P., Vlachopoulos.N., Graetzel. M. (1993). Conversion of light to electricity by cis-X_2-bis(2,2'-bipyridyl-4,4'-dicarboxylate)ruthenium(II) charge-transfer sensitizers (X = Cl-, Br-, I-, CN-, and SCN-) on nanocrystalline titanium dioxide electrodes. *American Chemical. Society, 115(14),* 6382-6390.

Nishantha, M. R., Yapa, Y. P. Y. P., & Perera, V.P.S. (2012). Sensitization of photoelectrochemical solar cells with a natural dye extracted from Kopsia flavida fruit. *ProcTech Sess*, *28*, 54–58.

Noor, M. M., Buraidah, M. H., Yusuf, S. N. F., Careem, M. A., Majid, S. R., & Arof, A. K. (2011). Performance of dye-sensitized solar cells with (PVDF-HFP)-KI-EC-PC electrolyte and different dye materials. *International Journal of Photoenergy*, *2011* 5 pages.

O'Regan., & Gratzel, M. (1991). A low-cost, high efficiency solar cell based on dye-sensitized colloidal TiO_2 films. *Nature*, *353,* 737-740.

Ogura, R. Y., Nakane, S., Morooka, M., Orihashi, M., Suzuki, Y., & Noda, K. (2009). High-performance dye-sensitized solar cell with a multiple dye system. *Applied Physics Letter, 94(7),* 073308.

University of Malaya

Ooyama, Y., Shimada, Y., Ishii, A., Ito, G., Kagawa, Y., Imae, I., Harima, Y. (2009). Photovoltaic performance of dye-sensitized solar cells based on a series of new-type donor-acceptor-conjugated sensitizer, benzofuro[2,3-c]oxazolo[4,5-a]carbazole fluorescent dyes. *Journal of Photochemistry and Photobiology A: Chemistry*, *203(2–3),* 177–185.

Ozawa, H., Shimizu, R., & Arakawa, H. (2012). Significant improvement in the conversion efficiency of black-dye-based dye-sensitized solar cells by cosensitization with organic dye. *Royal Society Chemistry Advances*, *2(8),* 3198–3200.

Oskam, G., Bergeron, B. V, Meyer, G. J., & Searson, P. C. (2001). Pseudohalogens for dye-sensitized TiO2 photoelectrochemical cells. *Physical Chemistry, B*, *105(29),* 6867–6873.

Pan, J., Benko, G., Xu, Y.H., Pascher, T., Sun, L.C., Sundstrom, V., & Polivka, T. (2002).Photoinduced electron transfer between a carotenoid and TiO2 nanoparticle. *American Chemical Society,124(46),* 13949–13957.

Pandey G.P., Kumar Y., & Hashmi S.A. (2011). Ionic liquid incorporated PEO based polymer electrolyte for electrical double layer capacitors: A comparative study with lithium and magnesium system, *Solid State Ionics*, *190,* 93-98.

Park, N. G., Chang, S. H., Van de Lagemaat, J., Kim, K. J., & Frank, A. J. (2000). Effect of cations on the open-circuit photovoltage and the charge-injection efficiency of dye-sensitized nanocrystalline rutile TiO2 films. *Bulletin of the Korean Chemical Society*, *21(10),* 985–988.

Patrocínio, A. O. T., Mizoguchi, S. K., Paterno, L. G., Garcia, C. G., & Iha, N. Y. M. (2009). Efficient and low cost devices for solar energy conversion : Efficiency and stability of some natural-dye-sensitized solar cells. Synthetic matel, *159,* 2342–2344.

Polo, S., Yukie, N., & Iha, M. (2006). Blue sensitizers for solar cells : Natural dyes from Calafate and Jaboticaba.*Solar Material and Solar Cells, 90,* 1936–1944.

Polu, A.R., Kumar, R., Chin. (2013). Preparation and characterization of PVA based solid polymer electrolytes for electrochemical cell applications.*Chinese Journal of Polymer Science. 31(4),* 641-648.

Rajendran, S., Mahendran, O., & Kannan, R. (2002). Ionic conductivity studies in composite solid polymer electrolytes based on methylmethacrylate. *Journal of Physics and Chemistry of Solids*, *63(2),* 303–307.

Sayama, K., Hara, K., Sugihara, H., Arakawa, H., Mori, N., Satsuki, M., Kitamura, T. (2000). Photosensitization of a porous TiO2 electrode with merocyanine dyes containing a carboxyl group and a long alkyl chain. *Chemical Communications*, *353*(13), *1173–1174*.

Shah. S., Buraidah, M.H., Teo, L.P., Careem, M.A., & Arof, A.K. (2016). Dye-sensitized solar cells with sequentially deposited anthocyanin and chlorophyll dye as sensitizers, *Optical and Quantum Electronics*, 4*8,* 219.

University of Malaya

Shanmukaraj, D., Wang, G. X., Murugan, R., & Liu, H. K. (2008). Ionic conductivity and electrochemical stability of poly(methylmethacrylate)-poly(ethylene oxide) blend-ceramic fillers composites. *Journal of Physics and Chemistry of Solids*, *69(1),* 243–248.

Shockley, W. & Queisser, H.J. (1961). Detailed Balance Limit of Efficiency of p-n Junction Solar Cells. *Journal of Applied Physics*, *32,*510-519.

Singh, P. K., Bhattacharya, B., Mehra, R.M., Rhee,H-W.(2011) .Plasticizer doped ionic liquid incorporated solid polymer electrolytes for photovoltaic application. *Current Applied Physics*, *11,* 616– 619.

Singh, P. K., Nagarale, R. K., Pandey, S. P., Rhee, H. W., & Bhattacharya, B. (2011). Present status of solid state photoelectrochemical solar cells and dye sensitized solar cells using PEO-based polymer electrolytes. *Advances in Natural Sciences: Nanoscience and Nanotechnology*, *2(2),* 23002.

Sima, C., Grigoriu, C., & Antohe, S. (2010). Comparison of the dye-sensitized solar cells performances based on transparent conductive ITO and FTO. *Thin Solid Films, 519,* 595–597.

Snaith, H. J., Moule, A. J., Klein, C., Meerholz, K., Friend, R. H., & Grätzel, M. (2007). Efficiency enhancements in solid-state hybrid solar cells via reduced charge recombination and increased light capture. *Nano Letters*, *7(11),* 3372–3376.

Sownthari, K., & Austin Suthanthiraraj, S. (2014). Preparation and properties of a gel polymer electrolyte system based on poly-ε-caprolactone containing 1-ethyl-3-methylimidazolium bis(trifluoromethylsulfonyl)imide. *Journal of Physics and Chemistry of Solids*, *75(6),* 746–751.

Suryanarayanan,V., Lee, K. M., Chen, J. G,. & Ho, K. C. (2009*).* High performance dye-sensitized solar cells containing 1-methyl-3-propyl imidazolinium iodide-effect of additives and solvent*s*. *Journal of Electroanalytical Chemistry*. *633(1),* 146-152.

Ruiz-Anchondo, T., Flores-Holguín, N., & Glossman-Mitnik, D. (2010). Natural carotenoids as nanomaterial precursors for molecular photovoltaics: A computational DFT study. *Molecules*, *15(7),* 4490–4510.

U.S. Energy Information Agency. (2013). International Energy Outlook 2013. Outlook *2013,* 312

Theerthagiri, J., Senthil, A. R., Madhavan, J., & Maiyalagan, T. (2015). Recent Progress in Non-Platinum Counter Electrode Materials for Dye-Sensitized Solar Cells. *ChemElectroChem, 2(7),* 928–945.

Vignarooban, K., Dissanayake, M. A. K. L., Albinsson, I., & Mellander, B.-E. (2014). Effect of TiO2 nano-filler and EC plasticizer on electrical and thermal properties of poly(ethylene oxide) (PEO) based solid polymer electrolytes. *Solid State Ion.*, 266, 25–28.

University of Malaya

Voigt, S., Orphal, J., & Burrows, J. P. (2002). The temperature and pressure dependence of the absorption cross-sections of NO2 in the 250-800 nm region measured by Fourier-transform spectroscopy. *Journal of Photochemistry and Photobiology A: Chemistry*, *149(1–3),* 1–7.

Wang, L., Shang, J., Hao, W., Jiang, S., Huang, S., Wang, T., Wang, J. (2014). A dye-sensitized visible light photocatalyst-$Bi_{24}O_{31}Cl_{10}$. *Scientific Reports*, 4, *7384.*

Wang, X. F., Kitao, O., Hosono, E., Zhou, H., Sasaki, S. ichi, & Tamiaki, H. (2010). TiO2- and ZnO-based solar cells using a chlorophyll a derivative sensitizer for light-harvesting and energy conversion. *Journal of Photochemistry and Photobiology A: Chemistry*, *210(2–3),* 145–152.

Wang, Z. S., Li, F. Y., & Huang, C. H. (2000). Highly efficient sensitization of nano crystalline TiO2 films with styryl benzothiazolium propylsulfonate. *Chemical Communication, 20,* 2063-2064.

Wongcharee, K., Meeyoo, V., & Chavadej, S. (2007). Dye-sensitized solar cell using natural dyes extracted from rosella and blue pea flowers. *Solar Energy Materials and Solar Cells*, *91(7),* 566–571.

Wu, J. *(2008).* High-performance polypyrrole nanoparticles counter electrode for dye-sensitized solar cells. *Journal of Power Sources, 181 (1),* 172–176.

Wu, J., Gross, A. & Yang, H. (2011). Shape and Composition-Controlled Platinum Alloy Nanocrystals Using Carbon Monoxide as Reducing Agent. *Nano Lett*ers, *11(2),*798–802.

Yamazaki, E., Murayama, M., Nishikawa, N., Hashimoto, N., Shoyama, M., Kurita, O. (2007). Utilization of natural carotenoids as photosensitizers for dye-sensitized solar cells. *Solar Energy*, *81(4),* 512–516.

Yu, Q.Y., Liao,J.Y., Zhou, S.M., Shen,Y., Liu, J.-M., Kuang, D. B. & Su, C.-Y.(2011). Effect of hydrocarbon chain length of disubstituted triphenyl-amine-based organic dyes on dye-sensitized solar cells. *Journal of American chemical society, 115(44),* 22002-22008.

Yun, J. H., Kim, I. K., Ng, Y. H., Wang, L., Amal, R. (2014). Optical modeling-assisted characterization of dyesensitized solar cells using TiO_2 nanotube arrays as photoanodes. *Beilstein Journal of Nanotechnology, 5,* 895–902.

Zaban, A.; Chen, S. G.; Chappel, S.; Gregg, B. A. (2000). Bilayer nanoporous electrodes for dye sensitized solar cells. *Chemical Communication,* 2231-2232.

Zhang, C. R. Liu, Z. J., Chen, Y. H., Chen, H. S., Wu, Y. Z., Yuan, L. H. (2009). DFT and TDDFT study on organic dye sensitizers D5, DST and DSS for solar cells. *Journal of Molecular Structure, Theochem, 899 (1-3),* 86–93.

Zhang, G., Bala, H., Cheng, Y., Shi, D., Lv, X., Yu, O., & Wang, P. (2009). High efficiency and stable dye-sensitized solar cells with an organic chromophore featuring a binary pi-conjugated spacer, *Chemical Commun*ication, *16,* 2198-2200.

University of Malaya

Zongo, S., Dhlamini, M. S., Kerasidou, A. P.,Beukes, P. Sahraoui, B., Maaza, M. (2015). Linear and nonlinear optical absorption characterization of natural laccaic acid dye, *Applied Physics B*, *Lasers and Optics, 15,* 6148-6153.

Zongo, S., Sanusi, K., Britton, J., Mthunzi, P., Nyokong, T., Maaza, M., Sahraoui, B. (2015). Nonlinear optical properties of natural laccaic acid dye studied using Z-scan technique, *Optical Materials*, *46,* 270–275.

University of Malaya

LIST OF PUBLICATION

Shah, S., Buraidah, M.H., Teo, L.P., Careem, M.A., & Arof, A.K. (2016). Dye-sensitized solar cells with sequentially deposited anthocyanin and chlorophyll dye as sensitizers, *Optical and Quantum Electronics*, 48, 219.

University of Malaya